ABSTRACT

Title of Document:	New Classes of Self-Assembled Structures in Nonpolar Solvents Hee Young Lee, Doctor of Philosophy, 2011
Directed By:	Professor Srinivasa R. Raghavan, Department of Chemical and Biomolecular Engineering

Many researchers have investigated the self-assembly of amphiphilic molecules in water into characteristic structures such as micelles and vesicles. In comparison, amphiphilic self-assembly in nonpolar organic liquids, which can be referred to as "reverse" self-assembly, is much less studied. In this dissertation, we describe a variety of new reverse self-assembled structures formed from amphiphilic molecules. Especially, we focus on long *reverse cylindrical structures* that can induce high viscosity, and *reverse vesicles*, i.e., hollow spherical containers surrounded by reverse bilayers. We expect that these reverse structures may be useful for applications such as gelling agents for fuels and oils, hosts for enzymatic reactions, and controlled release.

In the first part of this study, we describe the effects of adding inorganic salts to solutions of lecithin in nonpolar solvents. Lecithin is a zwitterionic, mono-unsaturated phospholipid that by itself forms reverse spherical micelles. Salts can be dissolved in these solvents in the presence of lecithin. Interestingly, salts of multivalent cations like calcium (Ca^{2+}), magnesium (Mg^{2+}), lanthanum (La^{3+}) and cerium (Ce^{3+}) greatly increase the viscosity of lecithin sols and transform them into optically transparent organogels. In comparison, monovalent cations or transition-metal cations have negligible effect on

reverse self-assembly. Based on data from small-angle neutron scattering (SANS), we show that gelation is accompanied by a transition from spherical micelles to cylindrical micelles/filaments. The varying abilities of different cations to induce gelation is shown to correlate with their binding tendencies to the phosphocholine headgroups of lecithin.

Next, we describe a class of photorheological (PR) fluids based on a nonpolar solvent such as cyclohexane. The rheological properties of these fluids can be reversibly tuned by UV and visible light. In order to create such PR fluids, reverse wormlike micelles of lecithin + sodium deoxycholate (SDC) are doped with a photoresponsive compound, spiropyran (SP). Spiropyrans can be reversibly converted from a closed-form (SP) to an open-form (MC) by UV and visible light, respectively. Initially, the reverse micelles in the lecithin/SDC/SP system are long and entangled, which makes the solution highly viscous. When exposed to UV light, the viscosity of these micellar solutions drops by a factor of 10. Conversely, when exposed to visible light, the viscosity recovers to approximately its initial value. We have found that this cycle between high and low viscosity states can be repeated more than 10 times.

Finally, we describe a new route to forming bilayered structures such as reverse vesicles and lamellae in organic solvents such as cyclohexane. This involves the combination of a saturated phospholipid, dimyristoyl phosphatidyl choline (DMPC) with an inorganic salt having either a trivalent cation like gadolinium (Gd^{3+}) or a divalent cation like calcium (Ca^{2+}). We find that the addition of the salt to DMPC solutions leads to either cylindrical aggregates or bilayered aggregates depending on the concentration of

the salt. The structural changes can be explained qualitatively in terms of changes in the molecular geometry (packing parameter) induced by the binding of cations to the headgroups of the phospholipid.

NEW CLASSES OF SELF-ASSEMBLED STRUCTURES IN NONPOLAR SOLVENTS

By

Hee Young Lee

Dissertation submitted to the Faculty of the Graduate School of the
University of Maryland, College Park, in partial fulfillment
of the requirements for the degree of
Doctor of Philosophy
2011

Advisory Committee:
Prof. Srinivasa R. Raghavan, Chair
Prof. Kyu Yong Choi
Prof. Ganesh Sriram
Prof. Robert M. Briber
Prof. Daniel E. Falvey

Dedication

This thesis is dedicated to Jesus Christ and my parents for their endless love, the enormous efforts they took for ensuring a good education for me.

Acknowledgements

First of all, I would like to thank my advisor Dr. Srinivasa Raghavan. He has not only been the research mentor on my scientific career, but the mentor on my entire outlook in life for the past six and half years. Due to his unlimited advice and support, I could have courage in the face of any adversities and overcome those during my graduate career. I owe all of my successes in graduate school to him.

Next, I would like to thank my sister, her husband and kid for their never-ending support. I have taken comfort from my sister and her husband words. Also whenever I met my nephew, he always made me smile. I believe in all them and I hope that I can inspire them in the way that they inspire me.

I would also like to thank my committee: Dr. Kyu Yong Choi, Dr. Ganesh Sriram, Dr. Robert M. Briber, and Dr. Daniel E. Falvey. All of them have provided me with valuable ideas and corrections that guided me to right direction for graduation.

I am infinitely grateful to all of my past and present fellow colleagues in Dr. Raghavan's lab: Jaeho Lee, Matt Dowling, Shihuang Tung, Bani Cipriano, Aimee Ketner, Rakesh Kumar, Kunshan Sun, Seung-Won Ko, Jennifer Hong, Elijah George, Chao Zhu, Oluwatosin Ogunsola, Peter Thomas, George Chacko, Khyati Tiwari, Vishal Javvaji, Veidhes Basrur, Hyuntaek Oh, Kaname Hashizaki, Kunqiang Jiang, Neville Fernades, Charles Kuo and Anande Bagal. Without you guys, my research would amount to nothing.

I certainly have to give a great deal of special thanks to my undergraduate students: Kevin Diehn and Adeeb Raziuddin. Without your help, I would not finish all of works.

TABLE OF CONTENTS

LIST OF TABLES

LIST OF FIGURES

Chapter 1

INTRODUCTION AND OVERVIEW

1.1. PROBLEM DESCRIPTION AND MOTIVATION

Many researchers have investigated a variety of amphiphiles (molecules with both hydrophilic and hydrophobic parts) that can self-assemble in aqueous solutions into characteristic nanostructures such as micelles and vesicles. These nanostructures can be quite useful for applications including detergency, controlled release, gelling agents, and templates for nanomaterials synthesis.[1-2] In direct contrast to water, which is a highly polar liquid, the self-assembly of amphiphilies can also occur in nonpolar organic solvents ("oils"), and it is termed "reverse self-assembly". The term "reverse" here refers to the nature of structures in oil where the amphiphiles are self-assembled in an opposite way to that of "normal" aggregates in water.[1-2] However, the study of such "reverse" self-assembly of amphiphiles in "oils" is much less developed.[3-5] For instance, the critical micelle concentration (CMC) or phase diagrams for amphiphiles in organic solvents have not been mapped out in detail as they have for water. Also, while a variety of amphiphiles are well-known for their self-assembly properties in water, only a limited number of amphiphiles have been investigated for their self-assembly in organic liquids. It should be noted that structures created by reverse self-assembly can also have a range of applications, such as in drug delivery, gelling fuels, and enzyme catalysis.[6-7]

In the context of reverse self-assembly, one system that has been well-studied is the lecithin/water/oil system.[8-11] The phospholipid, lecithin is known to form reverse

spherical micelles in oil. When a small amount of water is added, the spherical micelles grow into reverse wormlike micelles, i.e., long, flexible cylindrical chains. Recently, new routes for forming reverse wormlike micelles of lecithin have been found: instead of water, different additives such as bile salts or sucrose esters have been shown to achieve the same result.[12-14] These studies imply that a range of additives could influence the self-assembly of reverse systems. This is a topic that has seen very little study until recently and it is a point of emphasis in the present work. *The overall motivation for our work is the gap in knowledge with regard to reverse self-assemblies in oil*.

Apart from fundamental knowledge, we are also looking to create structures with unique properties. One aspect of interest is the ability to change self-assembly properties by shining light. In particular, we are interested in photorheological or PR fluids, which are fluids whose rheological properties can be tuned by light.[15-17] Previous examples of reversible PR fluids in nonpolar solvents have involved difficult organic synthesis.[16,18-19] Thus, another goal of our study is to create a simple reversible PR fluid in a nonpolar solvent based on reverse self-assembly.

1.2. PROPOSED APPROACH

In this dissertation, we report three distinct studies all centered around reverse self-assembly. These are depicted in **Figure 1.1** and briefly described below. Our focus in each case is on elucidating the link between molecular composition, nanoscale structure, and macroscopic (especially rheological) properties in these systems.

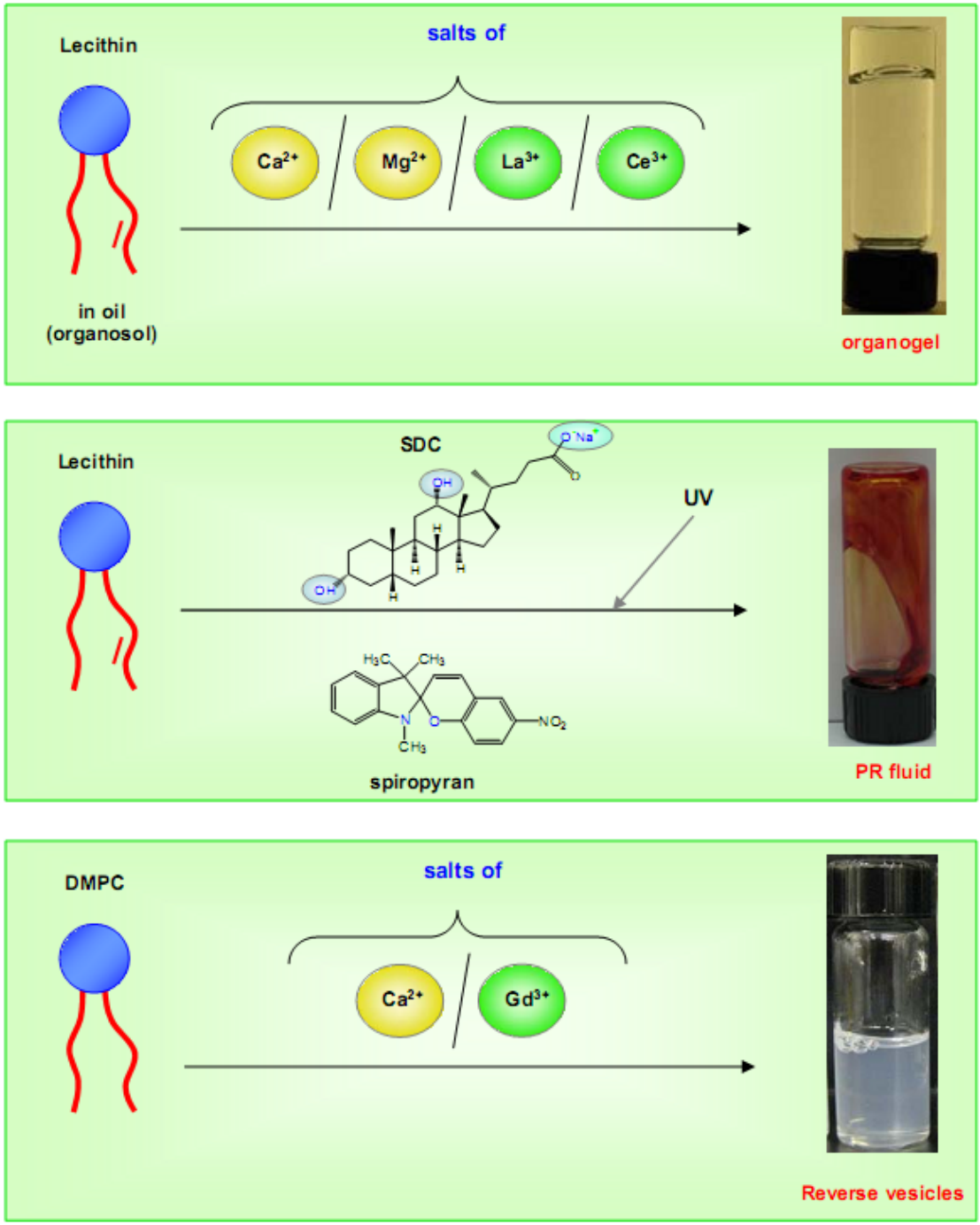

Figure 1.1. Amphiphilic systems investigated in this dissertation in the context of reverse self-assembly. The combination of an unsaturated phospholipid, lecithin along with multivalent cations produces organogels (top). The combination of lecithin with the bile salt, SDC, and a photoresponsive spiropyran creates PR fluids whose rheological properties can be tuned by light (middle). The combination of the saturated phospholipid, DMPC with multivalent cations produces reverse bilayered structures such as reverse vesicles (bottom).

1.2.1. Organogel Networks

First, in Chapter 3, we describe experiments on mixtures of lecithin with the simplest type of additive – common salts like sodium chloride, NaCl or calcium chloride, $CaCl_2$. We show that the type of cation matters: salts of multivalent cations like calcium (Ca^{2+}), magnesium (Mg^{2+}), lanthanum (La^{3+}) and cerium (Ce^{3+}) greatly increase the viscosity of lecithin sols and transform them into optically transparent organogels. Such gel-like behavior arises from entangled networks of cylindrical micelles or filaments in these lecithin/ion mixtures. The simplicity and low cost of this type of two-component gelator makes this system attractive for applications such as flammable fuel storage.

1.2.2. Reversible PR Fluids

Next, in Chapter 4, we describe a photorheological (PR) fluid based on mixtures of lecithin, the bile salt, sodium deoxycholate (SDC), and a photoresponsive compound, spiropyran (SP). The resulting micellar solutions show a reversible transition from a highly viscous to a moderately viscous state upon shining UV and visible light, respectively. This is the first example, to our knowledge, of a reversible non-aqueous PR fluid based on simple, commercially available components.

1.2.3. Reverse Bilayer Structures

Finally, in Chapter 5, we describe a new route to forming bilayered structures such as reverse vesicles and lamellae. These are induced by combining the saturated phospholipid, dimyristoyl phosphatidyl choline (DMPC), with an inorganic salt having

either a trivalent cation like gadolinium (Gd^{3+}) or a divalent cation like calcium (Ca^{2+}). Reverse vesicles are nanoscale liquid-filled containers, much like normal vesicles in water. To our knowledge, there are very few examples of such reverse vesicles in the literature,[20-27] and our study shows a simple, straightforward way to prepare them. These reverse vesicles could be used to encapsulate and deliver hydrophobic compounds such as flavor ingredients.

1.3. SIGNIFICANCE OF THIS WORK

The studies described in this dissertation are potentially significant from both scientific and practical standpoints. Firstly, from a scientific viewpoint, we provide new useful guidelines for controlling reverse self-assembly processes. It is well known that the driving force for the self-assembly in water is hydrophobic effect; however this may not be the key driving force in nonpolar liquids. Instead, forces like hydrogen bonding or ion-pair interactions may be more important, as shown by our work. This knowledge could help in achieving a more systematic understanding of reverse self-assembly and in guiding the design of new formulations. Also, nonpolar solvents may provide a platform to study certain interactions occurring in biological systems that may be disturbed by the presence of water (e.g., between lipids and metal ions).

Secondly, regarding the applications of the reverse systems that we have discovered, the organogels based on lecithin/cations could find application as hosts for enzymes or biomolecules due to their nontoxic nature. Also, the lecithin/cation organogelator can convert a liquid fuel like kerosene into a gel. Gelling of fuels is an

attractive way of ensuring their stability and safety during transportation and storage. As for PR fluids, their reversibility facilitates their use in emerging areas such as in the design of microscale robots or microfluidic valves. Finally, with regard to the reverse vesicles, they can have potential ability to encapsulate a variety of solutes and release these in a slow manner, thus serving as controlled-release carriers.

Chapter 2

BACKGROUND

This dissertation is concerned with "reverse" self-assembly in nonpolar organic liquids. In this chapter, we discuss both "reverse" and "normal" self-assembly and we describe the various structures that can be formed by self-assembly. Also, we introduce the molecules that can create these structures. We then describe the techniques that we will use to study these types of structures, such as rheology, small-angle neutron scattering (SANS) and dynamic light scattering (DLS).

2.1. SELF-ASSEMBLY OF AMPHIPHILES: NORMAL AND REVERSE

Amphiphilic molecules (also referred to as surfactants, detergents, or lipids) which have both distinct hydrophilic and hydrophobic portions can self-assemble in water or oil into characteristic structures. **Figure 2.1** shows that these molecules, which consist of hydrophilic heads shown in blue and hydrophobic tails shown in red, can form a variety of structures such as spherical micelles, cylinders and bilayer structures, in both water and . The process of spontaneous organization is referred to as self-assembly and it is governed by thermodynamics, i.e., it occurs because the system minimizes its Gibbs free energy in the process. Micelles can be formed only above a critical concentration of the amphiphile, referred to as the critical micelle concentration or CMC. The driving force for micellization is the gain in entropy of water molecules when the hydrophobes of the amphiphilies are shield from water molecules; this aspect is referred to as the hydrophobic effect.

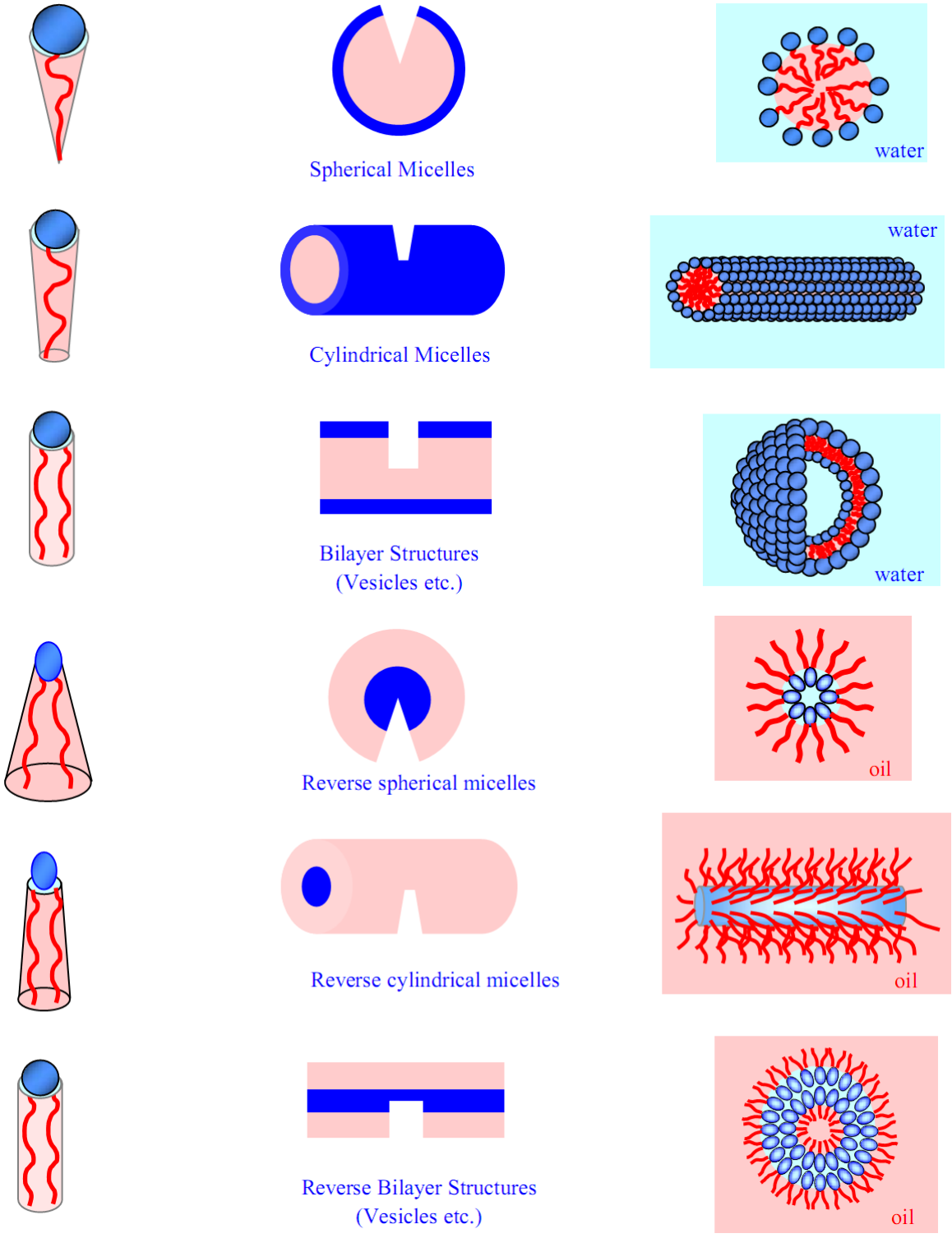

Figure 2.1. Schematics showing the connection between the self-assembled structures formed by amphiphiles in water and nonpolar liquids (oils) with the effective geometry of the amphiphilic molecules. The hydrophilic heads are shown in blue and the hydrophobic tails are depicted in red.

In addition to micelles, it is possible to form other structures through self-assembly. In order to logically explain the different aggregate shapes, we consider the net geometry of the amphiphilic molecules using a term called the critical packing parameter or CPP, which is defined as follows:[1]

$$\mathrm{CPP} = \frac{a_{\mathrm{tail}}}{a_{\mathrm{hg}}} \tag{2.1}$$

where a_{hg} and a_{tail} are the cross-sectional areas of the amphiphilic headgroup and tail respectively. As a_{hg} becomes larger, the aggregate has higher curvature, as shown in **Figure 2.1.** Thus, in water, a CPP around 1/3, corresponding to a cone shape, leads to spherical micelles. When the CPP increases to around ½ (truncated cone), it leads to cylindrical micelles. A further increase of a CPP to around 1 leads to the formation of bilayer structures (vesicles).

In the case of nonpolar organic liquids ("oils"), the shapes of self-assembled structures are also regulated by the CPP but in an opposite way. A CPP that is much greater than 1, corresponding to an inverse cone shape, leads to reverse spherical micelles, as shown in **Figure 2.1**. The term reverse refers to the inverse geometry of these micelles compared to the normal micelles in water. When the value of the CPP is slightly reduced, corresponding to an inverse truncated cone, reverse cylindrical micelles can form. Further decrease of the CPP will correspond once again to a cylinder shape, and this will induce reverse bilayer structures (including reverse vesicles). We will discuss reverse cylindrical micelles and vesicles in the following sections.

2.2. REVERSE CYLINDRICAL MICELLES

Normal cylindrical micelles have been formed by a variety of surfactants such as cationic, anionic, nonionic, and zwitterionic.[28-29] Similarly, reverse cylindrical micelles can be formed in oil, but there are only a few examples of the latter.[9,12-14] For example, the phospholipid, lecithin by itself can self-assemble to form reverse *spherical* micelles. When lecithin is mixed with additives such as water,[4,9,13,30] bile salts,[12-13] and sucrose fatty acid ester,[14] the spherical micelles grow to become reverse cylindrical micelles. It is believed that such additives bind to the headgroup of lecithin by forming hydrogen bonds, and thus the headgroup area of lecithin expand inducing the decrease of the CPP. Such decrease of the CPP in turn causes the spherical micelles to cylindrical micelle transition. When the cylinders are very long and flexible, they are described as wormlike chains, and the micelles are then termed "reverse wormlike micelles" or "reverse worms".

2.3. REVERSE BILAYER STRUCTURES

Bilayer structures can be formed by self-assembly of amphiphiles in water.[2,31] Among such bilayer structures, spherical vesicles are of particular interest.[1-2] The term "vesicle" refers to a spherical container in which the core contains water, while the outer shell consists of a bilayer with the hydrophobic portion shielded from water. The amphiphiles that compose the bilayer have the shape of a cylinder, i.e., a CPP around 1. While amphiphiles form vesicles at low concentration, they typically form a lamellar phase at high concentration.[32] Vesicles with only a single bilayer (or lamella) are called

unilamellar vesicles (ULVs), while vesicles with several concentric bilayers are called multilamellar vesicles (MLVs) and these are also referred to as “onions”.

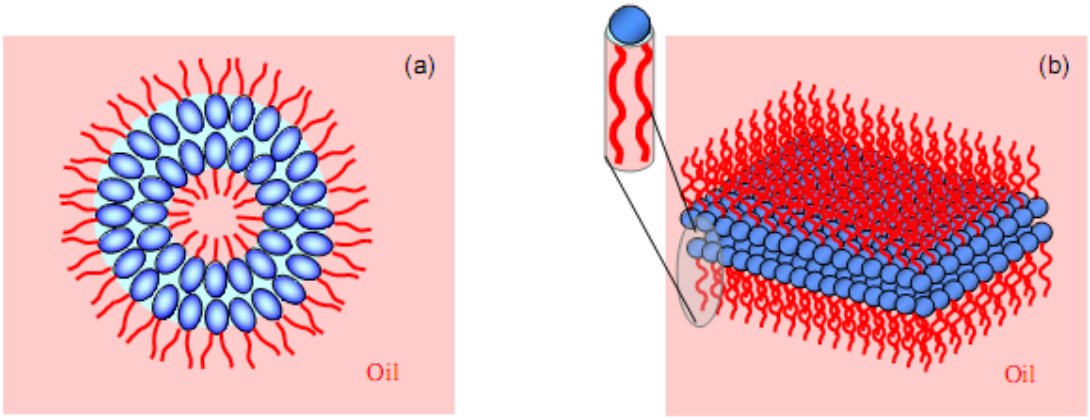

Figure 2.2. The structures of reverse bilayer structures such as a reverse spherical vesicle (a) and a reverse lamellar sheet (b). The amphiphilies are depicted with hydrophilic heads, shown in blue and hydrophobic tails, shown in red.

Similar to bilayer structures in water, bilayer structures can be formed in nonpolar solvents as well. The structure of reverse bilayer structures such as reverse vesicles and lamellar sheets in oil are shown in **Figure 2.2.** Note that the red tails of the amphiphiles are directed toward the oil phase and the blue heads are buried in the reverse bilayer. Compared to normal vesicles in water, there are only a handful of examples of reverse vesicles,[22,26,33] including those from amino acid derivatives,[22] sucrose esters,[21] and metallo-surfactants.[24] Most of these reverse vesicles are multilamellar and have a size in the micrometer scale, and their stability has been questionable. Thus, reverse vesicles do not find wide use at the moment, and there is still a lack of a general framework for their formation.

2.4. PHOSPHOLIPIDS

To make reverse cylindrical and bilayer structures in nonpolar solvents, we have used phospholipids as the key component. Phospholipids are well-known as the major constituents of most cell membranes. Membrane lipids tend to have a CPP close to 1 due to the large tail portion from two tails, and therefore, they self-assemble in water to form bilayer membranes. In our studies, we have mainly worked with two kinds of phospholipids. One is lecithin, which is a type of phosphatidylcholine (PC) obtained from natural sources such as egg yolk or soy beans. It has a head group composed of the positively charged choline part and the negatively charged phosphate part, i.e., the net molecule is zwitterionic. Of the two tails of lecithin, one is an unsaturated tail with two double bonds. In addition to lecithin, we have worked with dimyristoyl phosphatidyl choline (DMPC), which has two saturated C_{14} tails.

2.5. SPIROPYRANS

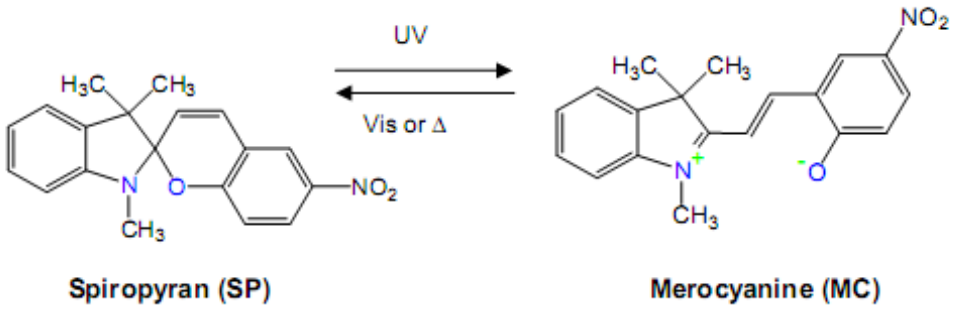

Figure 2.3. Spiropyran (closed ring) on the left converts to merocyanine (open ring) on the right via UV light, while the reverse occurs under visible light.

To create a new class of photorheological (PR) fluids, based on nonpolar solvents, we have doped reverse wormlike micelles with a photochromic compound, spiropyran.

Photochromism is the phenomena of reversible transformation of a chemical species between two forms that have different absorption spectra, resulting in color changes.[34-35] Spiropyrans are an extensively studied class of photochromic molecules.[36-39] They assume two types of structural forms (stereoisomers): a colorless form corresponding to the orthogonal "closed" structure (SP) and a colored form corresponding to the planar "open" structure (MC), as shown in **Figure 2.3**. The transition between these two forms can be induced by photo-irradiation or heat. For example, while the formation of MC can be induced by UV irradiation, that of SP can be recovered by visible light or heat. Such transition can be also affected by the solvent polarity.[40-41] Note that, while the SP form is nonpolar due to closed structure, the MC form is polar, with a zwitterionic character.

2.6. CHARACTERIZATION TECHNIQUES

2.6.1. Rheology

Rheology is formally defined as the study of flow and deformation in materials.[42] Rheological measurements provide important information on soft materials, specifically on the relation between microstructure and macroscopic properties. These measurements are typically performed under steady or dynamic shear. In steady shear, the sample is subjected to a constant shear-rate $\dot{\gamma}$ (e.g. by applying a continuous rotation at a fixed rate on a rotational instrument), and the response is measured as a shear-stress σ. The ratio of shear-stress σ to shear-rate $\dot{\gamma}$ is the (apparent) viscosity η. A plot of the viscosity vs. shear-rate $\dot{\gamma}$ is called the flow curve of the material.

Rheological experiments can also be conducted in dynamic or oscillatory shear, where a sinusoidal strain $\gamma = \gamma_0 \sin(\omega t)$ is applied to the sample. Here γ_0 is the strain-amplitude (i.e. the maximum applied deformation) and ω is the frequency of the oscillations. The sample response will be in the form of a sinusoidal stress $\sigma = \sigma_0 \sin(\omega t + \delta)$ which will be shifted by a phase angle δ with respect to the strain waveform. Using trigonometric identities, the stress waveform can be decomposed into two components, one in-phase with the strain and the other out-of-phase by 90°:

$$\sigma = G'\gamma_0 \sin(\omega t) + G''\gamma_0 \cos(\omega t) \tag{2.2}$$

where G' is the **Elastic** or **Storage Modulus** and G'' is the **Viscous** or **Loss Modulus**.

The physical interpretations of the two moduli are as follows. The elastic modulus G' is the in-phase component of the stress and provides information about the elastic nature of the material. Since elastic behavior implies the storage of deformational energy, this parameter is also called the storage modulus. The viscous modulus G'', on the other hand, is the out-of-phase component of the stress and characterizes the viscous nature of the material. Since viscous deformation results in the dissipation of energy, G'' is also called the loss modulus. For these properties to be meaningful, the dynamic rheological measurements must be made in the "*linear viscoelastic*" (LVE) regime of the sample. This means that the stress must be linearly proportional to the imposed strain (i.e., moduli independent of strain amplitude). In that case, the elastic and viscous moduli are only functions of the frequency of oscillations ω, and are true material functions. A log-log

plot of the moduli vs. frequency, i.e. $G'(\omega)$ and $G''(\omega)$, is called the frequency spectrum of the material and represents a signature of the material microstructure.

The important advantage of dynamic shear is that it allows us to characterize microstructures without disrupting them in the process. The net deformation imposed on the sample is minimal because the experiments are restricted to small strain amplitudes within the LVE regime of the sample. As a result, the linear viscoelastic moduli reflect the microstructures present in the sample at rest. This is to be contrasted with steady shear, where the material functions are always obtained under flow conditions corresponding to relatively drastic deformations. We can therefore correlate dynamic rheological parameters to static microstructures, and parameters under steady shear to flow-induced changes in microstructure.

2.6.2. Small-Angle Neutron Scattering (SANS)

Scattering techniques are invaluable probes of micro- and nanostructure in soft materials.[43] Their basic principle is that the intensity of scattered radiation from a structured fluid is a function of the size, shape, and interactions of the "particles" present. Small-angle neutron scattering (SANS) is the technique of choice in studying our samples as it probes structure over size scales around a few nm. In SANS, the contrast between the solvent and the "particles" is achieved by switching the hydrogen in the solvent with deuterium, e.g., using D_2O instead of H_2O. SANS requires a nuclear reactor to generate neutrons and we are fortunate to have one of the premier SANS facilities nearby at the National Institute of Standards and Technology (NIST) in Gaithersburg, MD.

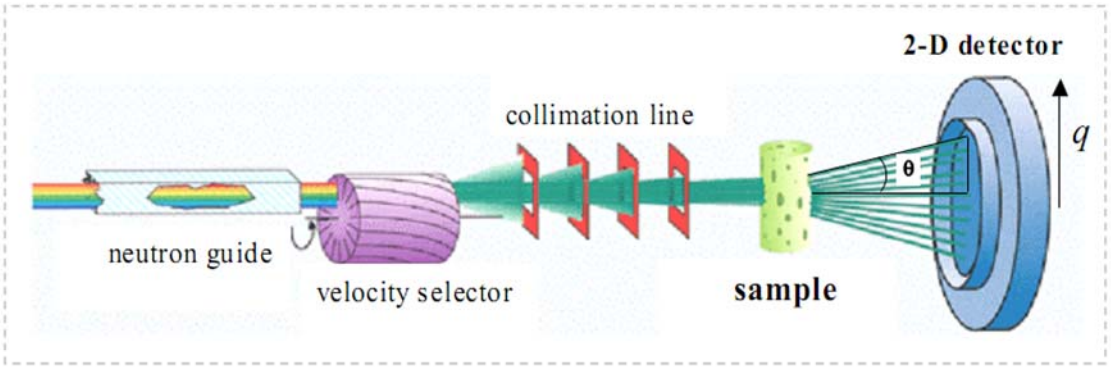

Figure 2.4. Schematic of a SANS experiment.

The basic geometry of a SANS experiment is shown in **Figure 2.4**. Neutrons from a nuclear reactor pass through a velocity selector set for a particular wavelength and wavelength spread. These neutrons then pass through several collimating lenses and into the sample placed in the sample chamber. The neutrons scattered by the sample are collected on a 2-D detector. Using calibration standards, this 2-D data is corrected and placed on an absolute scale. It is then converted into a plot of scattered intensity I vs. wave vector q by spherical averaging. The wave vector is defined as:[43]

$$q = \frac{4\pi}{\lambda}\sin\left(\frac{\theta}{2}\right) \tag{2.3}$$

Here, λ is the wavelength of the incident radiation and θ is the scattering angle. q can be considered an inverse length scale, with high q pertaining to small scales, and vice versa.

The SANS intensity $I(q)$ from a structured fluid containing n_p particles per unit volume can be expressed in the following manner:

$$I(q) = n_p \cdot P(q) \cdot S(q) \tag{2.4}$$

where $P(q)$ is called the form factor and $S(q)$ the structure factor. $P(q)$ is the scattering that arises from intraparticle interference, which is a function of the particle size and shape. $S(q)$ arises from interparticle interactions and thereby reflects the spatial arrangement of particles. When the particles are in dilute solution or are non-interacting, the structure factor $S(q) \rightarrow 1$ and the SANS intensity $I(q)$ can then be modeled purely in terms of the form factor $P(q)$. Form factors for different particle geometries are known and these can be fit to the data to obtain structural information about the particles.

2.6.3. UV-Vis Spectroscopy

UV-Vis absorption spectroscopy is an analytical technique used to study molecules that absorb radiation in the ultraviolet (200~400 nm) and visible (400~800) regions of the electromagnetic spectrum. When a molecule absorbs radiation in the UV-Vis range, the absorbed energy generally moves electrons into higher energy levels. The molecule does not absorb energy continuously throughout the spectral range because the absorbed energy is quantized; i.e., the molecule will absorb only at wavelengths that provide that exact amount of energy necessary to promote electrons to higher energy levels.[44] Each compound will thus have a unique UV-Vis spectrum. UV-Vis can thus serve as an analytical technique, especially for compounds that have an aromatic group.

A typical UV-Vis experiment is done with a solution of low solute concentration, which is then placed in a cuvette into the sample cell of a UV-Vis spectrometer. Light is broken down into its component wavelengths in the spectrometer and passed through the sample. The absorption intensity is measured for each wavelength and a UV-Vis

spectrum (plot of absorbance vs. wavelength) is produced for the sample. UV-Vis spectroscopy can be used as a quantitative analytical method to determine the concentration of the solute. This is done using the Beer-Lambert law.

$$A = \varepsilon \cdot c \cdot l \tag{2.5}$$

where A is the measured absorbance at a particular wavelength, c is the concentration of the solute in mol/L, l is the path length of the sample, and ε is the molar extinction coefficient or molar absorptivity at that wavelength.

2.6.4. Dynamic Light Scattering (DLS)

Static scattering techniques such as SANS provide important information about the quiescent structure in complex fluids. Dynamic scattering techniques have a complementary role in that they probe structural relaxations and dynamics. In particular, dynamic light scattering (DLS) probes the Brownian motion of particles in the fluid. This method can give a reliable estimate of particle size under certain limiting conditions. In a DLS experiment, the fluctuating intensity of light scattered from the sample is recorded at a certain angle θ. The fluctuations are then correlated to yield the intensity autocorrelation function $g^{(2)}(q, \tau)$ vs. the correlation time τ :[45]

$$g^{(2)}(q,\tau) = \frac{\langle I(q,t)I(q,t+\tau)\rangle}{\langle I(q,t)^2\rangle} \tag{2.6}$$

Note that in light scattering, the definition of the wave vector is slightly modified as:

$$q = \frac{4\pi n}{\lambda}\sin\left(\frac{\theta}{2}\right) \tag{2.7}$$

where n is the refractive index of the medium. The relevance of q in DLS is that structural relaxations are probed over length scales on the order of q^{-1}.

The measured intensity autocorrelation function $g^{(2)}(q, \tau)$ can be converted into an electric field autocorrelation function $g^{(1)}(q, \tau)$ through the Siegert relation:

$$g^{(2)}(q,\tau) = 1 + f\left|g^{(1)}(q,\tau)\right|^2 \tag{2.8}$$

Here, f is an adjustable parameter called the coherence factor that depends on the instrument geometry. For a dilute solution of monodisperse spherical particles, the electric-field autocorrelation function is a single exponential whose time decay is determined by the translational diffusion coefficient of the particle D:

$$g^{(1)}(q,\tau) = \exp\left(-Dq^2\tau\right) \tag{2.9}$$

From the measured diffusion coefficient, the particle size can be obtained by the Stokes-Einstein equation:

$$D = \frac{k_B T}{6\pi\eta R_h} \tag{2.10}$$

where k_B is the Boltzmann constant, T the absolute temperature and η the viscosity of the solvent (assumed to be a Newtonian liquid). The size obtained from DLS is the *hydrodynamic radius* R_h. The hydrodynamic size is the bare particle size along with any solvation layer.

Chapter 3

MULTIVALENT CATIONS AS EFFICIENT GELATORS OF LECITHIN ORGANOSOLS

The results presented in this chapter have been published in the following journal article: Hee-Young Lee, Kevin K. Diehn, Seung-Won Ko, Shih-Huang Tung, and Srinivasa R. Raghavan, "*Can simple salts influence self-assembly in oil? Multivalent cations as efficient gelators of lecithin organosols*" Langmuir **2010**, *26*, 13831-13838.

3.1. INTRODUCTION

In this chapter, we describe our first study, which puts forward a new route to form organogels in nonpolar organic liquids ("oils"). It is well known that amphiphilic molecules can self-assemble in water into characteristic structures such as micelles and vesicles.[1,32] Aqueous self-assembly of amphiphiles is recognized to be driven primarily by hydrophobic interactions, but electrostatic interactions are known to play an important role as well. For example, take the effect of added salt (e.g., NaCl or $CaCl_2$) on a cationic surfactant in water with respect to either the critical micelle concentration (CMC) of the surfactant or the size and shape of its micelles. It is known that salts reduce the CMC and that they can induce a transition from spherical to long cylindrical micelles (also called wormlike micelles or worms[46]). Such effects are easily rationalized in terms of classical electrostatic theory:[1,32] the salt ions reduce the electrostatic repulsions between the

cationic surfactant headgroups (in effect decreasing the Debye screening length), which facilitates micellization and assembly into cylindrical structures. Salt effects on aqueous self-assembly thus have a consistent physical basis.

Self-assembly of amphiphilies can also occur in non-polar organic liquids ("oils" for short) and this is referred to as "reverse" self-assembly.[1,32] Compared to self-assembly in water, much less is known about reverse self-assembly;[3-5] for instance, amphiphiles in oil may or may not have a well-defined CMC. Phase diagrams for amphiphiles in organic solvents have also not been mapped out in detail as they have for water. An additional issue that has rarely been considered is the effect of adding salt to a solution (organosol) of an amphiphile in oil. *Will the added salt influence the assembly process?* At first, this question may seem nonsensical because practical experience teaches us that salts like NaCl and $CaCl_2$ cannot be dissolved in oil. However, in reality, small amounts of salts can be dissolved in oil when an amphiphile is also present. This is akin to solubilizing small amounts of oil in water containing surfactant micelles (the resulting mixture is then termed a microemulsion).[32] In fact, in a similar vein, hydrophilic molecules such as enzymes have previously been solubilized in oil within the interior of reverse micelles.[47-48] If salts can indeed be introduced into oil, the interesting question then is whether the type of salt (e.g., NaCl vs. $CaCl_2$) would matter. The present study will show a class of oil-based systems in which the type of salt critically impacts self-assembly.

The systems reported in this Chapter are solutions in nonpolar organic liquids of the two-tailed phospholipid, lecithin along with a simple inorganic salt. Lecithin is well-

known to form reverse spherical or ellipsoidal micelles in a range of organic liquids.[4,11] Previous research has also shown that the addition of water in small amounts to a lecithin organosol can induce the growth of reverse micelles from spheres to long, flexible cylindrical micelles (worms).[9,11] More recently, we have reported that the same effect can also be induced by the addition of bile salts, which are a class of naturally occurring steroidal amphiphiles. These bile salts were insoluble if directly added to oils, but could be solubilized in the presence of lecithin.[12-13] In the present study, we shifted our attention from bile salts to more common, inorganic salts. We find that the latter can also be solubilized in lecithin organosols – and moreover, the type and concentration of salt control self-assembly in these mixtures.

The most interesting result from our study is the strong specificity of the salt cation: in particular, divalent cations from Group 2 of the Periodic Table (specifically Ca^{2+}, Mg^{2+}) and trivalent lanthanides (La^{3+} and Ce^{3+}) convert lecithin organosols into optically transparent organogels. This macroscopic change in sample rheology is driven by a transition from spherical reverse micelles to cylindrical filaments,[11-12] as we shall show using small-angle neutron scattering (SANS). In comparison, monovalent cations from Group 1 of the Periodic Table (e.g., Na^{+}, K^{+}) have negligible influence on self-assembly. Also, transition metal cations, both divalent (e.g., Co^{2+}, Cu^{2+}, Cd^{2+}) and trivalent (e.g., Fe^{3+}) have no effect. The striking results we observe with divalent cations and lanthanoids are consistent with their strong propensity to bind with the phosphocholine headgroups of lecithin.[49-54] Lipid-ion interactions have been well-studied

in aqueous media and we will use those findings in putting together a mechanism for the multivalent cation-induced transformation of lecithin reverse micelles.

Apart from its fundamental implications, the formation of organogels by combining lecithin and a Ca^{2+} (or similar) salt may also be of technological interest. Weiss and co-workers[55-56] have emphasized the search for the "simplest types" of organogelators. While a few simple gelators have been found (e.g., certain long-chain n-alkanes[56]), most current molecular gelators are complex organic structures that need to be synthesized in the laboratory.[55-57] In comparison, the lecithin/Ca^{2+} combination may be among the simplest and least expensive options for organogelation. Note that lecithin is a widely available, low-cost, food-grade material. Lecithin/Ca^{2+} gels are likely to be biocompatible and nontoxic; they could even be used safely to make home-made gels out of edible oils. Gels can be formed with organic fuels such as kerosene and gasoline and at less than 4 wt% overall of the additives. We have also been able to make lecithin/Ca^{2+} organogels isothermally, i.e., without the use of heat, and also without employing any mixing or shear (see Figure 3.6 later). These gels are indefinitely stable at room temperature, but can be converted to sols by heat or by addition of a polar co-solvent. Lecithin/salt mixtures are thus a class of organogelators with much practical potential.

3.2. EXPERIMENTAL SECTION

Materials. Soybean lecithin (95% purity) was purchased from Avanti Polar Lipids. The following anhydrous (> 99.99% purity) salts were purchased from Sigma-Aldrich: magnesium chloride ($MgCl_2$), calcium chloride ($CaCl_2$), strontium chloride ($SrCl_2$),

barium chloride ($BaCl_2$), lanthanum chloride ($LaCl_3$) and cerium chloride ($CeCl_3$). All other salts were purchased from Sigma-Aldrich, J. T Baker or Fisher-Scientific. Toluene, silicone oil, and dimethyl sulfoxide (DMSO) were purchased from Fisher-Scientific. All other solvents (at least > 99% purity) were purchased from Sigma-Aldrich.

Sample Preparation. Mixed solutions containing lecithin and salts were prepared as follows. Lecithin and salt were separately dissolved in methanol (or in some cases, ethanol) to form 100 mM stock solutions. Samples of particular compositions were prepared by mixing the stock solutions. The solvent was removed by drying the samples under a fume hood for 24 h and then in a vacuum oven for at least 48 h. The final samples were obtained by adding the organic solvent, followed by stirring and heating at 60 °C till the solutions became transparent and homogeneous. The above procedure ensured the removal of any residual water from the sample, and thereby facilitated reproducible sample preparation. An alternate procedure that does not involve any heating or stirring is described in the Results section (see Figure 3.6).

Rheological Studies. Steady and dynamic rheological experiments were performed on an AR2000 stress controlled rheometer (TA Instruments). Samples were run on cone-and plate geometries (20 mm dia / 2° cone-angle or 40 mm dia / 4° cone-angle). The plates were equipped with Peltier-based temperature control and all samples were studied at 25 ± 0.1°C. A solvent trap was used to minimize evaporation of solvent. Dynamic frequency spectra were conducted in the linear viscoelastic regime of the samples, as determined from dynamic strain sweep measurements. For steady-shear experiments,

sufficient time was allowed before data collection at each shear rate to ensure that the viscosity reached its steady-state value.

Small Angle Neutron Scattering (SANS). SANS measurements were made on the NG-7 and NG-3 (30 m) beamlines at NIST in Gaithersburg, MD. Neutrons with a wavelength of 6 Å were selected. Three sample-detector distances were used to obtain data over a range of wave vectors from 0.004 to 0.4 $Å^{-1}$. Samples were studied in 1 mm or 2 mm quartz cells at 25°C. Scattering spectra were corrected and placed on an absolute scale using NIST calibration standards. The data are shown as plots of the absolute intensity I versus the wave vector $q = 4\pi\sin(\theta/2)/\lambda$, where λ is the wavelength of incident neutrons and θ the scattering angle. Modeling of SANS data was conducted using software modules provided by NIST to be used with the IGOR graphing package.[58]

SANS Modeling. For dilute solutions of non-interacting scatterers, the SANS intensity $I(q)$ can be modeled purely in terms of the form factor $P(q)$ of the scatterers. In this study, we consider form factor models for ellipsoids and cylinders. In the expressions below, $\Delta\rho$ is the difference in scattering length density between the aggregate and the solvent, so that $(\Delta\rho)^2$ is the scattering contrast.

Ellipsoids. The form factor $P(q)$ for ellipsoids of revolution with minor and major axes R_a and R_b is given by:[59]

$$P(q) = (\Delta\rho)^2 \left(\frac{4}{3}\pi R_a R_b^2\right)^2 \int_0^1 \left[3\frac{(\sin x - x\cos x)}{x^3}\right]^2 d\mu \qquad (3.1)$$

where $x = q\sqrt{\mu^2 R_b^2 + R_a^2\left(1-\mu^2\right)}$. Here α is the cosine of the angle between the scattering vector q and the symmetry axis of the ellipsoid.

Cylinders. The form factor $P(q)$ for cylinders of radius R_c and length L is given by:[59]

$$P(q) = \left(\Delta\rho\right)^2 \left(\pi R_c{}^2 L\right)^2 \int_0^{\pi/2} \left[F(q,\alpha)\right]^2 \sin\alpha \, d\alpha \tag{3.2}$$

where
$$F(q,\alpha) = \frac{J_1\left(qR_c \sin\alpha\right)}{\left(qR_c \sin\alpha\right)} \cdot \frac{\sin\left(qL\cos\alpha/2\right)}{\left(qL\cos\alpha/2\right)} \tag{3.3}$$

Here α is the angle between the cylinder axis and the scattering vector q and $J_1(x)$ is the first-order Bessel function of the first kind. If the cylinders are polydisperse, the form factor has to be averaged over the length distribution in the following manner:

$$P(q) = \int f(L) \cdot P\left(q,L\right)\, dL \tag{3.4}$$

where $P(q, L)$ is the form factor for a cylinder of length L (eq 2). The polydispersity in cylinder length $f(L)$ can be accounted for by a Schultz distribution:

$$f(L) = \left(\frac{p+1}{L_0}\right)^{z+1} \frac{L^z}{\Gamma\left(z+1\right)} \exp\left(-\left(z+1\right)\frac{L}{L_0}\right) \tag{3.5}$$

In the above expression, L_0 is the average cylinder length and Γ is the gamma function. The polydispersity p_d is given by:

$$p_d = \frac{1}{\sqrt{z+1}} \tag{3.6}$$

3.3. RESULTS AND DISCUSSION

3.3.1. Phase Behavior and Rheology of the Gels

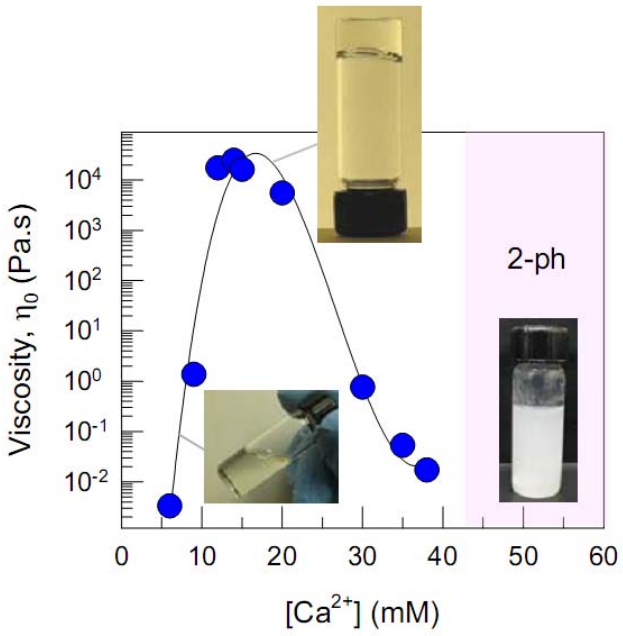

Figure 3.1. Zero shear viscosity η_0 of solutions in *n*-decane containing 40 mM lecithin and varying amounts of [Ca^{2+}]. Photographs of three samples at different [Ca^{2+}] are also shown. At low [Ca^{2+}], the solutions have a low viscosity. Around 14 mM [Ca^{2+}], the viscosity peaks and the sample is gel-like: it flows very slowly in the inverted vial. Beyond the peak, the viscosity drops precipitously, and around 40 mM [Ca^{2+}] the sample becomes turbid, indicative of phase-separation.

We first present results for mixtures of lecithin and anhydrous calcium chloride ($CaCl_2$) in *n*-decane. **Figure 3.1** shows the zero-shear viscosity η_0 of solutions containing 40 mM of lecithin and various Ca^{2+} concentrations. At a [Ca^{2+}] of 5 mM or lower, the viscosity is close to that of the solvent. At slightly higher [Ca^{2+}], the viscosity rapidly increases. Samples with about 12-15 mM of Ca^{2+} are gel-like and their viscosities are about a million times higher than that of the solvent. The photograph of such a sample is shown in the figure and one can see that the sample flows very slowly in the inverted

vial, indicating gel-like behavior. Note also that this organogel is optically clear and colorless; also there is no indication of any solid precipitate – i.e., the salt is completely dissolved in the sample. The other interesting result from Figure 3.1 is that the viscosity shows a non-monotonic behavior – it peaks around 14 mM Ca^{2+} and then falls sharply. By about 40 mM Ca^{2+}, the sample has reverted to a thin, clear liquid with a viscosity close to that of the solvent. Thereafter, around 43 mM Ca^{2+}, the sample becomes turbid while staying homogeneous. The turbidity is indicative of large structures and/or phase separation. Samples in this regime were not studied further.

Next, we used rheological techniques to characterize the gel-like lecithin/Ca^{2+} samples at intermediate [Ca^{2+}]. **Figure 3.2a** shows the dynamic rheological response (elastic G' and viscous G'' moduli as functions of frequency ω) of a sample containing 40 mM lecithin and 14 mM Ca^{2+}, which corresponds to the viscosity peak in Figure 3.1. Both moduli show weak frequency dependence, with G' dominating over G'' across the entire frequency range – thus, the sample response is mostly elastic. The gap between the moduli narrows at low frequencies, but the curves but do not intersect – this indicates that the relaxation time of the sample is very high and falls outside the window of timescales probed by rheometry. The above response can be characterized as *gel-like*. A true gel would show frequency-independent moduli over the entire frequency range, reflecting infinite values of relaxation time and viscosity.[42,60] Here, the moduli have a weak frequency dependence and so the sample does relax, albeit very slowly. In turn, the sample has a finite but high viscosity, as can be seen from its steady-shear response (**Figure 3.2b**), which reveals a plateau in the apparent viscosity at low shear-rates. The

plateau value is the zero-shear viscosity η_0 and it is the value plotted in Figure 3.1. All lecithin/Ca^{2+} samples we studied had finite η_0 values. Increasing the gelator concentration increased the value of η_0 but did not qualitatively change the nature of the rheological response. An example is shown in Figure 3.2b for a sample with 80 mM lecithin and 28 mM Ca^{2+}, which has a η_0 of about 10^5 Pa.s.

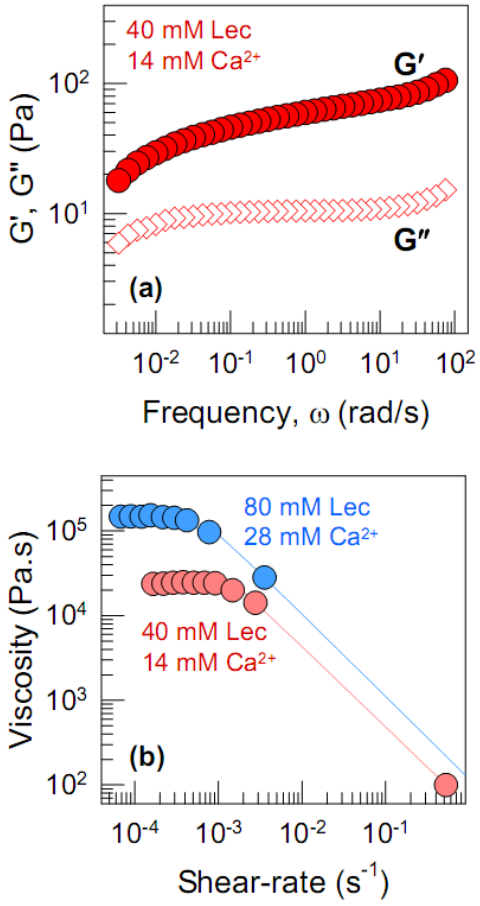

Figure 3.2. Dynamic and steady-shear rheology at 25°C of gel-like lecithin-Ca^{2+} samples in *n*-decane. In (a), dynamic data (elastic modulus G' and viscous modulus G'' as functions of frequency ω) are shown for a sample of 40 mM lecithin + 14 mM Ca^{2+}. In (b) steady-shear data (viscosity vs. shear-rate) are shown for the above sample as well as for a sample containing 80 mM lecithin + 28 mM Ca^{2+}.

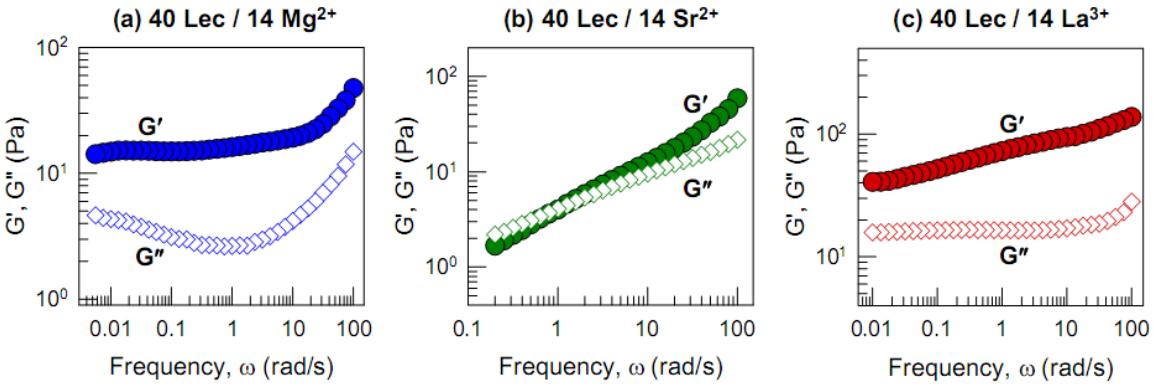

Figure 3.3. Rheology of lecithin samples containing various multivalent cations. Dynamic frequency sweeps are shown for samples in *n*-decane containing 40 mM of lecithin and 14 mM of (a) Mg^{2+} ; (b) Sr^{2+}; and (c) La^{3+}. All samples are highly viscous or gel-like.

The above data show that lecithin/Ca^{2+} mixtures can convert organic liquids like *n*-decane into clear, gel-like samples (we will refer to these samples as "organogels" for convenience). A lecithin:Ca^{2+} molar ratio of 40:14 or about 3:1 seems to be optimal for inducing gelation. The next question is whether other salts can also serve as organogelators. We examined a number of other salts in this context, and selected rheological results are shown in **Figure 3.3** for the same solvent (*n*-decane) and for concentrations of 40 mM lecithin and 14 mM of the respective salts. First, we evaluated other divalent cations along Group II of the periodic table. Both $MgCl_2$ and $SrCl_2$ were able to modulate fluid viscosity. The dynamic response of the Mg^{2+} sample (**Figure 3.3a**) is distinctly gel-like, with a flat (frequency-independent) *G′* and a non-monotonic *G″*. Here also, the moduli do not intersect over the frequency range, indicating that the relaxation time is very high. In comparison, the Sr^{2+} sample **(Figure 3.3b**) shows a viscoelastic response, with *G′* and *G″* intersecting around a frequency of 1 rad/s. In other words, Sr^{2+} is a weaker gelator; to attain gel-like behavior, higher lecithin and Sr^{2+}

concentrations are necessary. In addition to the Group II cations, we were also able to produce organogels using salts of the rare-earth lanthanoids, specifically, La^{3+} and Ce^{3+}. **Figure 3.3c** shows the rheology of a lecithin/$LaCl_3$ sample, which again shows gel-like behavior with G' exceeding G'' over the frequency range.

	Compound	Phase / State
Cations: Monovalent (Group 1, alkali metals)	NaCl	Sols
	KCl	Sols
	CsCl	Sols
Cations: Divalent (Group 2, alkaline earth metals)	$MgCl_2$	**Gels**
	$CaCl_2$	**Gels**
	$SrCl_2$	**Gels**
	$CaBr_2$	**Gels**
	CaI_2	**Gels**
Cations: Divalent (Transition Metals)	$CoCl_2$	Sols
	$CuCl_2$	Sols
	$CdCl_2$	Sols
Cations: Trivalent (Lanthanides)	$LaCl_3$	**Gels**
	$CeCl_3$	**Gels**
Cations: Trivalent (Others)	$FeCl_3$	Sols
	$AlCl_3$	Sols

*All studies done in n-decane with 20-40 mM of lecithin and 0-40 mM of salt. Sol vs. gel distinguished visually.

Table 3.1. The ability of various salts to convert lecithin organosols into orgnogels.

Table 3.1 collects our observations with various salts contrasting those that induce organogelation and those that do not. The majority of these observations were made in the solvent *n*-decane, although similar trends hold for other solvents as well (see below). We found two broad patterns of behavior. In the case of gel-inducing salts, the

progression with increasing salt concentration, as depicted in Figure 3.1, is from sol to gel, then back to near-sol (down the viscosity peak), and then the formation of a turbid, low-viscosity phase. This pattern was found for Mg^{2+}, Ca^{2+}, Sr^{2+}, La^{3+}, and Ce^{3+}. In the case of Ca^{2+}, in addition to $CaCl_2$, we also examined anhydrous $CaBr_2$ and CaI_2 – gels were formed with these other anions as well. The second pattern of behavior was observed with the rest of the salts, which included salts of Na^+, K^+, Cs^+, Co^{2+}, Cu^{2+}, Cd^{2+}, Al^{3+} and Fe^{3+}. All these salts had no effect on the viscosity of lecithin organosols. When their concentration was raised too high, these salts could no longer be solubilized and excess (undissolved) salt precipitated out as solid crystals.

Organogels using the combination of lecithin and a multivalent cation like Ca^{2+} could be produced in a range of non-polar organic solvents. In addition to *n*-decane, we have prepared gels in other *n*-alkanes, iso-alkanes, cyclohexane, fuels like kerosene, fatty acid esters, and aromatic solvents like styrene and divinyl benzene. The most efficient gelation (viscosity maximum) occurred at a lecithin:Ca^{2+} molar ratio ~ 3:1 in all the solvents we studied. All gels were indefinitely stable at room temperature. Gelation did not occur, however, in polar organic solvents like ethanol or other alkanols. In these polar solvents, the salts dissolved directly without the need for lecithin. Thus, for gelation to occur, the salt must be insoluble in the neat solvent and must dissolve only in the presence of lecithin. This ensures that the salt ions are sequestered in the polar regions of the reverse micellar structures formed by lecithin.

We have also characterized the temperature-dependent response of lecithin/Ca^{2+} organogels. As has been noted earlier, organogels tend to "melt", i.e., their rheology undergoes a sharp change (gel to sol transition) at a distinct temperature.[55,61] In contrast, wormlike micelles show a more gradual change in their rheological properties – the viscosity and relaxation time show a steady, exponential decrease over the range of temperatures.[13,61] In the case of lecithin/Ca^{2+} organogels, the temperature response is a hybrid of the above (data not shown). On heating, the gels do not "melt" at a distinct temperature; rather, their zero-shear viscosity gradually drops. However, the dynamic response has the same qualitative behavior as that shown in Figure 3.2a, i.e., the relaxation time remains long and outside the window of frequencies probed. These aspects require more careful study and are not discussed further in this paper.

We should also point out that all the salts we studied were anhydrous, and so the results are not due to residual or bound water, either in the lecithin or in the salts. In our earlier study, we had determined using ^{1}H NMR that residual water is present in lecithin at a molar ratio of 0.9:1 (water:lecithin).[12-13] However, if we added lecithin alone to an organic solvent, the solution was nonviscous. Also, bound water cannot explain why we see organogel formation only with certain cations and not others.

3.3.2. Microstructure of the Gels from SANS

Next, we describe the results of SANS experiments on lecithin/Ca^{2+} organogels. These were conducted using deuterated cyclohexane as the solvent and with the lecithin concentration fixed at 20 mM. $I(q)$ plots are shown in **Figure 3.4a** for four different

[Ca^{2+}]; for clarity, the same plots are shown scaled by factors of 5 in **Figure 3.4b**. In Figure 3.4a, we observe that the intensity at low q increases substantially as [Ca^{2+}] is increased. For samples with no Ca^{2+} or very low Ca^{2+}, the intensity tends to a plateau at low q. In contrast, the sample with 7.2 mM Ca^{2+} shows a power-law behavior close to $I \sim q^{-1}$ (slope of –1 on the log-log plot) at low q, which is the scaling relationship expected for rod-like structures.[13,59] Finally, note the slight drop in intensity at the lowest q for the 14.4 mM Ca^{2+} sample compared to the 7.2 mM one. The same data also shows more of a deviation from the $I \sim q^{-1}$ scaling at low q.

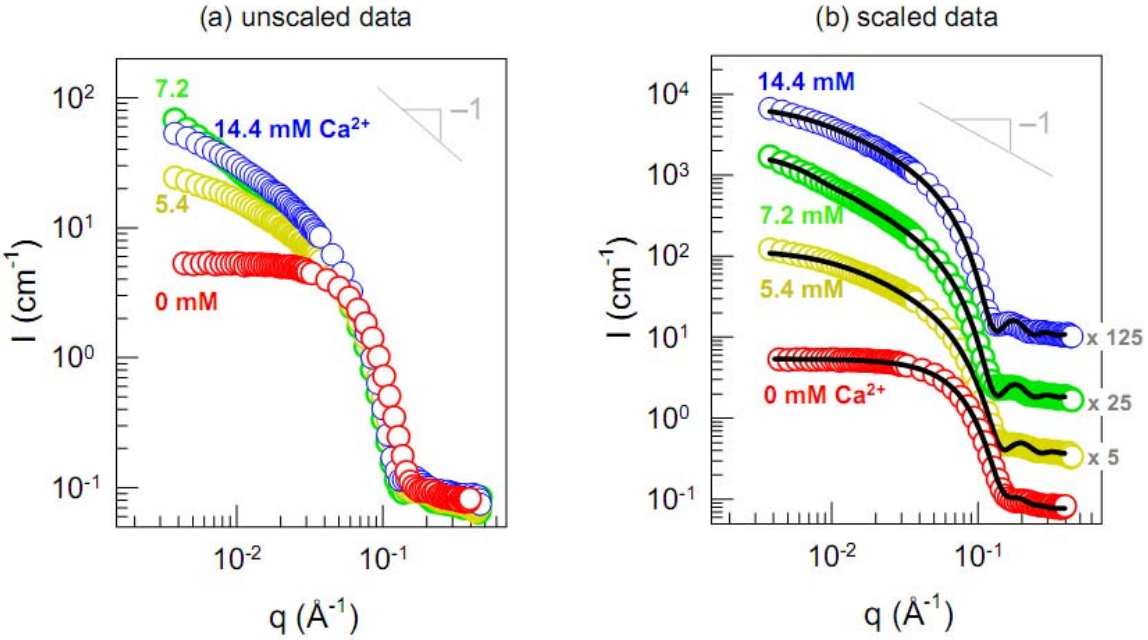

Figure 3.4. SANS spectra (intensity I vs. wave-vector q) for samples in deuterated cyclohexane containing 20 mM lecithin and various concentrations of Ca^{2+}. In (a) the data are plotted on an absolute scale. Note that the intensity at low q increases from 0 to 5.4 to 7.2 mM Ca^{2+} and then decreases slightly for 14.4 mM Ca^{2+}. The same data are plotted in (b) with the different curves separated by factors of 5. Model fits (solid lines) are shown through each curve in this plot.

We have fitted form-factor models (described in the Experimental section) to the above SANS data, and the fits are shown in **Figure 3.4b** as solid lines through the data. Parameters from the modeling are shown in **Table 3.2**. For the 20 mM lecithin / no Ca^{2+} sample, the data admits to an oblate ellipsoid model (eq 3.1) with nearly identical major and minor axes (33.4 Å and 21.5 Å respectively), indicating that the micelles are close to spherical.[12] For the other plots, a model for polydisperse cylinders (eq 3.2 – 3.6) is used. From the fit parameters, we note a small but distinct increase in the cylinder radius with increasing [Ca^{2+}]: from 25.8 Å for 5.4 mM Ca^{2+} to 28.9 Å for 14.4 mM Ca^{2+}. Also, the average cylinder length sharply increases initially (from 131 Å for 5.4 mM Ca^{2+} to 748 Å for 7.2 mM Ca^{2+}) but then drops to 246 Å for the 14.4 mM Ca^{2+} sample. In other words, the cylinder length seems to increase and then decrease with [Ca^{2+}], which reflects the trend in the zero-shear viscosity as a function of [Ca^{2+}] (Figure 3.1).

Sample	**Model type**	**Ellipsoid param.**		**Polydisperse cylinder param.**		
Lec / Ca^{2+} (mM)		R_a (Å)	R_b (Å)	R_c (Å)	L_0 (Å)	p_d
20 / 0	Ellipsoids (oblate)	21.5	33.4			
20 / 5.4	Polydisp cylinders			25.8	131.2 ± 2.3	0.99
20 / 7.2	Polydisp cylinders			28.1	776.6 ± 7.6	0.24
20 / 14.4	Polydisp cylinders			28.9	245.9 ± 3.1	0.84

Table 3.2. SANS model parameters obtained by fitting data in Figure 3.4.

It is useful to compare the above parameters with those for lecithin-bile salt reverse wormlike micelles from our earlier study.[12] There also, the $I(q)$ for the lecithin-only sample was modeled as ellipsoids, and the model parameters were nearly identical. As the micelles grew upon addition of bile salt from ellipsoids to cylinders and then to

worms, the cylinder radius remained constant and identical to that of the minor axis of the ellipsoid (22 Å). The average length of the cylinders, on the other hand, increased monotonically with the bile salt concentration. Here, we find that the cylinder radius is not a constant as a function of [Ca^{2+}] while the length increases and then decreases. Still, there is a clear correlation between the Ca^{2+} induced growth of cylindrical structures and the increase in sample viscosity (organogelation).

3.3.3. Mechanism for Ion-Induced Gelation

We now discuss the differences between various cations in inducing gelation of lecithin organosols. Ion-specific effects have been known for a long time in organogelators. One of the earliest examples was napalm, the material used in flame-throwers in World War II, which were a mixture of gasoline and the aluminum complex of di-fatty acids.[62-64] A variety of other organic molecules have been reported to act as organogelators when complexed with metal ions such as Fe(III) or Cu(II).[65-67] In most of these studies, the complex was first created by reacting the organic molecule and the metal salt (in water or other solvent). The isolated product of such a reaction (i.e., the complex) was then combined with organic liquids under heat and stirring to create organogels. The metal ions for these complexes were chosen based on earlier binding/co-ordination studies, and thus only specific ions were investigated. For example, tetracarboxylate amphiphiles were complexed only with Cu(II)[65] while phosphonate esters were complexed with Fe(III) or aluminum.[66-67]

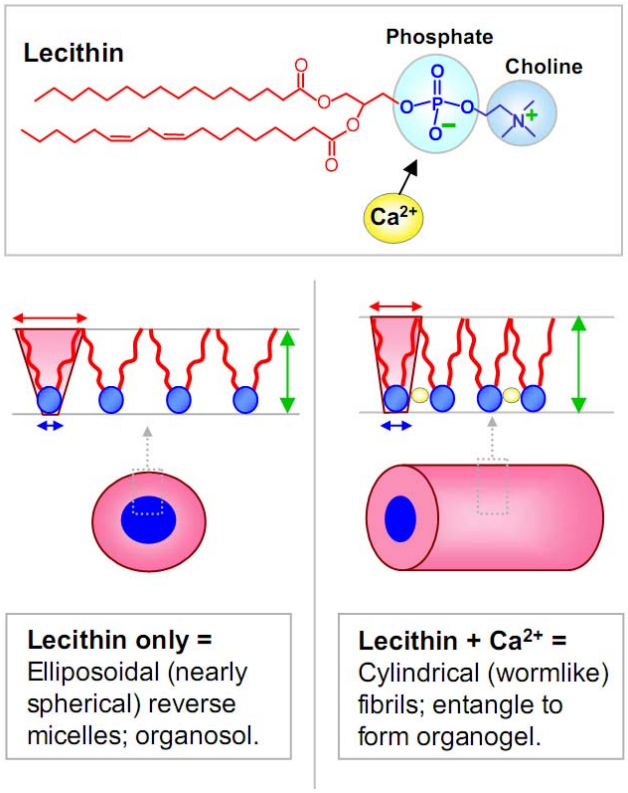

Figure 3.5. Effect of cations like Ca^{2+} on assemblies of lecithin in organic solvents. The top panel shows the structure of lecithin, highlighting its phosphocholine headgroup. Cations like Ca^{2+} bind to the phosphate portion of the headgroup. The bottom left panel reveals that lecithin alone has a conical shape and forms discrete, spherical reverse micelles. The bottom right panel depicts Ca^{2+} ions (yellow spheres) binding to lecithin (one ion per two lipids), causing the headgroup area a_{hg} (blue arrow) to expand. The lipid tails also become more straightened, causing the tail area a_{tail} (red arrow) to shrink and the micelle radius (green arrow) to increase. The molecular geometry becomes more like a truncated cone and in turn, the assemblies transform into cylindrical (wormlike) fibrils, thereby converting the sample into an organogel.

In the present study, we use a mixture of lecithin + salt as the organogelator, i.e., we do not first isolate a complex of lecithin and a given cation. Also, we observe gel formation by a variety of cations, including alkaline earth metals (Group 2 of the periodic table) and rare earth metals from the lanthanide series (La^{3+}, Ce^{3+}). The common feature of all these ions is their tendency to bind to the phosphocholine headgroups of lecithin.

Over the years, numerous studies have examined the interactions between ions and phospholipids in water, both by experiments[49-52] and by simulations.[53-54] Their findings are highly pertinent here as well, even though our solvents are non-polar organics. Akutsu and Seelig found that the binding affinity of cations to zwitterionic phospholipids followed the order $Na^+ < Ca^{2+} < La^{3+}$.[49] These ions were shown to associate with the polar headgroups of the lipids, and more specifically with the phosphate (negatively charged) portion of the headgroups, as illustrated in **Figure 3.5.**[49,53] Other studies have confirmed and extended the above order of cation-binding affinities. For example, Marra and Israelachvili showed that Ca^{2+} binds stronger to bilayers of phosphatidylcholines than Mg^{2+}, whereas the binding of monovalent cations like Na^+ was negligible.[51] Furthermore, in a study on micelles formed by C_8-lecithin in water, Huang *et al*. reported that Ca^{2+} had the strongest binding affinity among divalent cations.[52] Also, the affinity of La^{3+} was comparable to that of Ca^{2+} but lower than that of Ce^{3+}.[52]

Our results on organogel formation correlate with the binding affinities described above. Organogelation is induced by Ca^{2+}, but not by Na^+ or other monovalent cations. The elastic moduli G' of the gels are higher for Ca^{2+} than for Mg^{2+} or Sr^{2+}, indicating that Ca^{2+} is probably the most efficient gelator among the divalent ions (Figures 3.2, 3.3). Also, the G' values for La^{3+} are comparable to those for Ca^{2+}, indicating that La^{3+} is also a very efficient gelator. Taken together, our results reveal a systematic connection between phospholipid-cation binding and organogelation. Why should this be so? We know from SANS that cations like Ca^{2+} transform spherical micelles of lecithin into long cylindrical filaments. This suggests a scenario where binding of Ca^{2+} *alters the net*

geometry of the lipids to one favoring cylindrical structures at the expense of spherical ones. Similar arguments have been put forth in our earlier studies on lecithin/bile salt mixtures.[12-13]

The geometry argument can be framed in terms of the critical packing parameter $p = a_{tail}/a_{hg}$ where a_{tail} and a_{hg} are the cross-sectional areas of the tail and headgroup, respectively.[1] Lecithin alone tends to have a p much greater than 1 in oil, implying an inverse cone shape – and this accordingly leads to near-spherical reverse micelles (**Figure 3.5**). A reduction in p due to either an expansion of the headgroup area a_{hg} or a shrinking of the tail area a_{tail} would transform the geometry into a truncated cone shape – and this would drive a transition from spheres to cylinders. It is possible for the binding of Ca^{2+} or other cations to expand the lipid headgroup area a_{hg}, especially since the multivalent nature of the cations implies simultaneous binding to more than one lipid at the same time (see below). A second effect that could be important is that cation binding forces the lipid molecules together, which makes the lipid tails more densely packed and ordered.[53,68-69] The tails are effectively forced into a more straightened configuration and in turn, the average cross-sectional area a_{tail} per lipid may decrease.[68-69] Thus, cation binding may simultaneously affect both a_{tail} and a_{hg} in ways that cause a decrease in p, and this is shown in Figure 3.5.

We should point out here that the cylindrical chains or filaments in lecithin/ion mixtures appear to be very different from the reverse wormlike micelles seen, for example, in lecithin/water[9,11] or similar systems.[12-14,70-71] A characteristic property of

wormlike micelles (both normal and reverse) is that they are "living" polymers: they rapidly break and re-form due to exchange of amphiphiles between neighboring chains.[11,46] In the limit where the timescale for breaking τ_{br} is much shorter than that for chain reptation τ_{rep}, the micellar sample behaves as a viscoelastic Maxwell fluid with a single relaxation time.[11,46] Lecithin/ion samples, on the other hand, are gel-like (elastic), not viscoelastic, and their rheology is quite different from that of a Maxwell fluid. The most likely explanation is that the cylindrical lecithin/ion chains have very different dynamics. The binding of cations like Ca^{2+} to the phospholipids is expected to be quite strong and this will hinder the facile exchange of lipids between the chains. Therefore, chain breaking and reforming will be significantly retarded (i.e., τ_{br} will be very large) – in effect, the chains will behave more like "dead" (static) rather than "living" (dynamic) polymers. The entanglement of these long, robust chains can in turn lead to a quasi-permanent gel network. The chains could still relax by reptation, but they are apparently long enough to ensure that such relaxation is very slow (the reptation time $\tau_{rep} \sim L^3$ where L is the contour length[13,46]). This explains why a distinct relaxation time could not be detected within the frequency window of dynamic rheological experiments.

We also noted an increase in the radius of the cylinders with increasing $[Ca^{2+}]$ from the SANS modeling. This was in contrast to the results for lecithin/bile salt mixtures where the micellar radius was independent of the bile salt concentration. The growing cylinder radius is likely due to the straightening of lipid tails mentioned above. Note that lecithin has a *cis*-unsaturation in one tail, which implies a kink in that tail. When cations bind to lecithin, the lipid molecules are brought closer and this is believed to make the

tails straighter and more ordered.[53,68-69] In the case of lipid bilayers in water, tail ordering has been shown to increase the bilayer thickness.[69] The same effect can increase the effective thickness of cylindrical chains in our lecithin/ion mixtures, and this is also shown schematically in Figure 3.5.

Lastly, past studies on lipid-ion binding can also help to explain the maximum in viscosity vs. [Ca^{2+}] seen in Figure 3.1. Both experiments and simulations have shown that the binding between Ca^{2+} and zwitterionic phospholipids is optimized at a molar ratio of approximately 2 lipids per Ca^{2+} ion.[50,53] The viscosity maximum likely reflects this binding stoichiometry. As seen from Figure 3.1, the viscosity increases to a peak at a molar ratio of ~ 2.8 lipids per Ca^{2+} ion, which is close to the optimal binding ratio mentioned above. At this point, every Ca^{2+} ion is expected to be bound strongly to lipid headgroups, and this seems to correlate with the longest cylindrical micelles/filaments. Beyond this point, the presence of excess [Ca^{2+}] seems to cause a decrease in the cylinder length (as inferred from SANS modeling, Table 3.2), which correlates with the decrease in viscosity. The precise reason for the cylinder shortening is not clear, but it is possible that the excess Ca^{2+} stabilizes the end-caps of cylindrical filaments (more end-caps means shorter filaments). Alternately, excess Ca^{2+}, if still weakly bound to the lipid headgroups, may drive a transition from cylinders to reverse bilayers.

Lipid-ion mixtures in oil are thus analogous in many ways to the same mixtures in water. Oil-based systems may provide an ideal platform to study the interactions of biologically relevant lipids with various ions. From the viewpoint of organogelation, the

potency of lipid-ion gelators could be further improved by rational choice of the lipid. For example, anionic lipids like phosphatidylglycerols (PG) or phosphatidylserines (PS) are known to interact much more strongly with cations like Ca^{2+} compared to the zwitterionic phosphatidylcholines.[68,72] Also, lipid-ion interactions are considerably stronger when the lipids are in their gel (frozen) state rather than in their fluid state.[51] Thus, we predict that an anionic lipid with long saturated tails, when combined with Ca^{2+}, could act as a very potent organogelator. Of course, the lecithin/Ca^{2+} system is probably by far the most suitable for applications, as discussed below.

3.3.4. Room-Temperature Gelling and Ungelling

Finally, we wish to briefly discuss the potential utility of using lecithin/ion mixtures as organogelators. It is worth reiterating how simple and inexpensive this combination is. Lecithin is a food-grade phospholipid that is frequently used in commercial and food products; it can be easily purchased in kilogram quantities. Lecithin/Ca^{2+} mixtures will be biocompatible and non-toxic – they should thus be safe and gentle on the environment. The combination of low cost and biocompatibility could make these mixtures attractive for applications. One potential application is to convert liquid fuels into gels so as to store and transport these flammable liquids in a safe manner that avoids problems of fuel leakage or spillage. However, a problem in many such applications is that the introduction of gelator into the solvent requires heat and/or shear. The gelator is usually mixed as a powder with the solvent and the mixture is heated to dissolve the gelator. To facilitate applications, it would be imperative to avoid this heating step.[66-67]

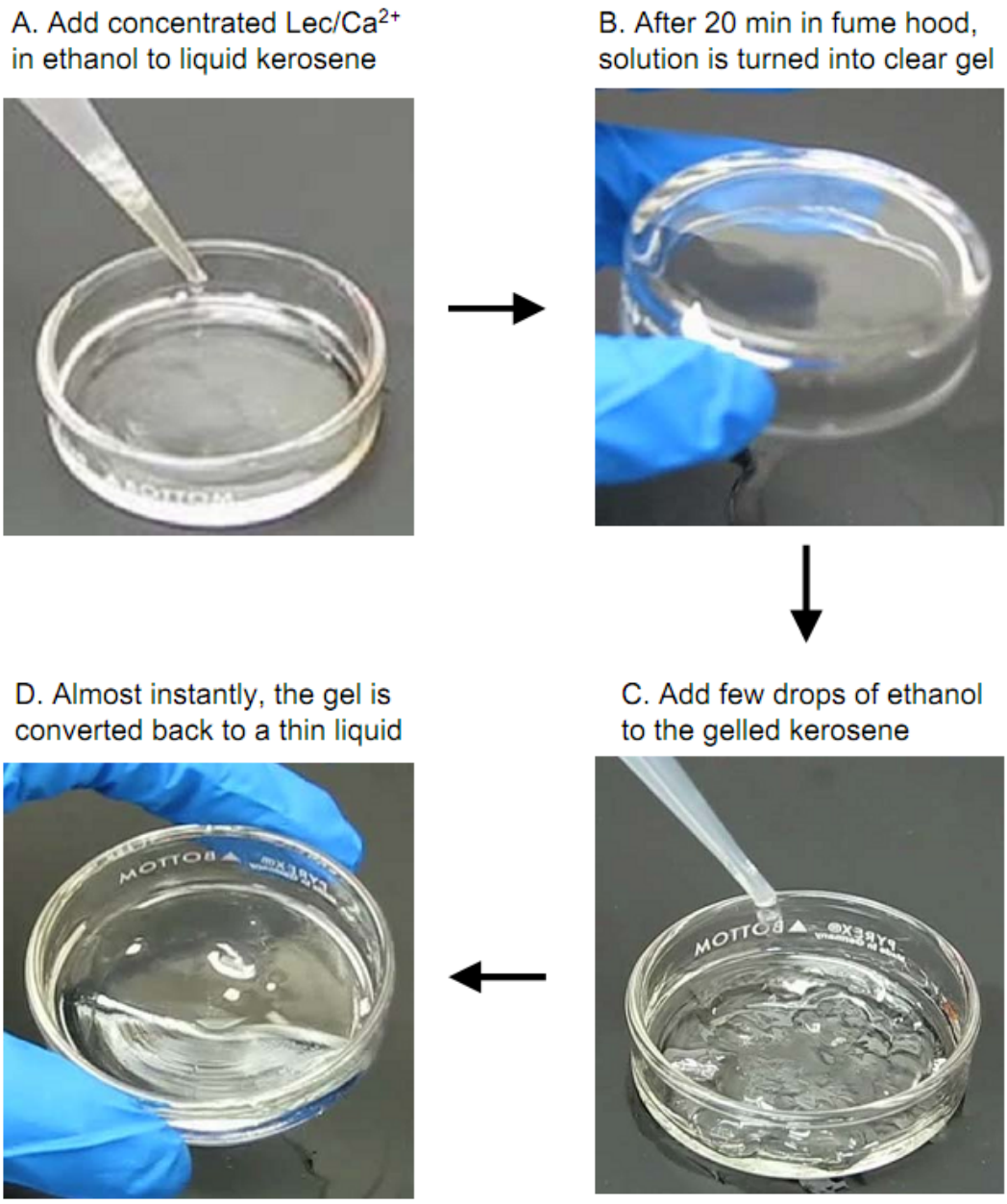

Figure 3.6. Isothermal gelling and ungelling of kerosene. In Panel A, kerosene is poured into a petri dish, and to this a concentrated solution of the gelator (lecithin + $CaCl_2$ in ethanol in a molar ratio 20:7) is added. The petri dish is then placed in a fume hood for 20 min, whereupon the volatile solvent, ethanol, evaporates – and in turn, the liquid kerosene is converted into a clear organogel (Panel B). The petri dish is inverted to show the gel-like nature of the sample. To ungel (liquefy) this sample, in Panel C, a few drops of ethanol are added. Almost instantly, the gel is converted back to a thin liquid, as can be confirmed from the tilted petri dish (Panel D).

In this context, we describe how one could make gels using lecithin/Ca^{2+} without using either heat or shear, as shown by the photographs in **Figure 3.6**. The solvent we have used is kerosene, a typical liquid fuel. We took about 5 mL of kerosene in a petri dish, as shown in Panel A. Separately, we prepared a concentrated solution of lecithin and $CaCl_2$ in ethanol (620 mM lecithin + 220 mM Ca^{2+}), with the molar ratio roughly corresponding to the optimum for gelation. Because lecithin/Ca^{2+} does not gel ethanol, the ethanol solution was a thin liquid. Using a pipette, we added a small amount of the above solution to the kerosene such that the overall [lecithin] and [Ca^{2+}] in dry kerosene would be 40 mM and 14 mM respectively. The petri dish was then placed in a fume hood, where the relatively volatile ethanol was allowed to evaporate. The evaporation was complete in about 20 min. In turn, the kerosene was converted into a clear gel, and this is shown in Panel B. Neither heat nor any mixing or stirring were employed during the above gelation process. Also, instead of placing the sample in a fume hood, one could remove the ethanol in a few seconds by passing nitrogen gas over the sample.

An additional aspect is the ability to liquefy (ungel) the above kerosene gel as desired. For example, fuels may be stored in gelled form when not in use but may need to be liquefied for eventual use. Ungelling of lecithin/Ca^{2+} gels can also be done without heat or shear, and this is also depicted in Figure 3.6. Here, we make use of the fact that an alcohol like ethanol is a good solvent for calcium salts and can thus act as an ungelling agent. In Panel C, we add a few drops of ethanol to the gelled kerosene. Instantly, we can observe the ethanol infiltrate the gel and begin to liquefy it. The petri dish is gently shaken for a few seconds within which time the gel is completely converted into a sol

(Panel D). Thus, ungelling can be readily accomplished at ambient temperature. The above gelling-ungelling cycle can be repeated: if the ethanol added to ungel is removed in a fume hood, the sample will be gelled again.

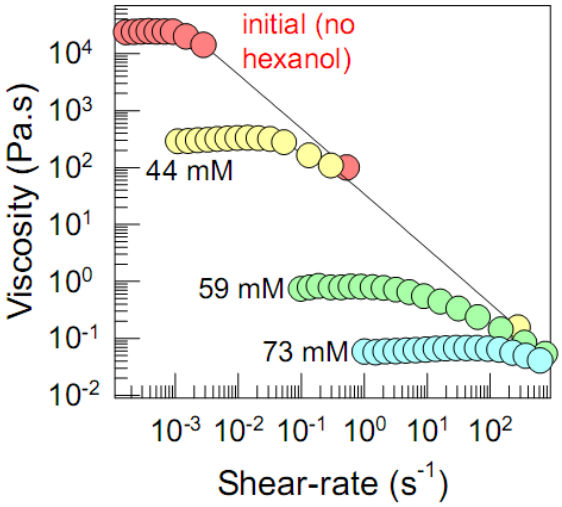

Figure 3.7. Ungelling of a lecithin/Ca^{2+} gel by addition of *n*-hexanol. Viscosity vs. shear-rate plots are shown for a sample of 40 mM lecithin + 14 mM Ca^{2+} in *n*-decane after addition of different amounts of *n*-hexanol (indicated beside each plot).

The ungelling of lecithin/Ca^{2+} gels by alcohols can also be accomplished in a controlled manner (i.e., to intermediate extents). We have studied such ungelling using steady-shear rheology. For this purpose it is convenient to use a less-volatile alcohol such as *n*-hexanol. **Figure 3.7** shows data for a gel composed of 40 mM lecithin and 14 mM Ca^{2+} in *n*-decane, to which we add increasing amounts of *n*-hexanol. Addition of *n*-hexanol causes the zero-shear viscosity η_0 to be lowered systematically. With about 73 mM of *n*-hexanol, the η_0 is reduced by more than five orders of magnitude and the sample response becomes nearly Newtonian (i.e., a constant viscosity over the range of shear rates). Thus, a very small amount of alcohol is enough to liquefy the gel.

3.4. CONCLUSIONS

This study has demonstrated that simple inorganic salts can modulate the self-assembly of phospholipids like lecithin in organic solvents. Salt effects vary with the cation, and in particular, strong effect are found in the case of the divalent alkaline earth metals (Ca^{2+} and Mg2+) and trivalent lanthanoids, lanthanum (La^{3+}) and cerium (Ce^{3+}). These multivalent cations bind with the phosphocholine headgroups of lecithin and induce a transition from spherical reverse micelles to cylindrical fibrils. The fibrils have diameters ranging from ca. 4 to 6 nm while their lengths are expected to exceed several hundred nm. These fibrils behave like “dead”, rather than “living” polymers; that is, they do not undergo frequent long, robust fibrils gives rise to a quasi-permanent gel network. Lecithin/ion gels can be formed in a variety of non-polar organic solvents, and gel formation can be induced without hear or shear by use of a volatile cosolvent. These gels can also subsequently be ungelled by the addition of polar solvents like alcohols.

Chapter 4

REVERSIBLE PHOTORHEOLOGICAL FLUIDS BASED ON SPIROPYRAN-DOPED REVERSE MICELLES

4.1. INTRODUCTION

In this chapter, we describe reversible photorheological (PR) fluids based on nonpolar solvents. Several research groups, including ours, have been interested in fluids whose rheological properties as viscosity can be altered by irradiation with light.[15-16] Such fluids can be termed photorheological or PR fluids.[17,73] Most PR fluids studied to-date have employed complicated photoresponsive molecules, such as photo-surfactants,[15,74-76] polymers,[77-79] or organogelators.[16,18-19,80] In order to make such photoresponsive molecules, skills in organic synthesis are essential, which may not be available to physical scientists or engineers. Recently, the capability of these PR fluids for use in microscale robots or microfluidic systems has come into sight. For such applications, it is important to have PR fluids that can be prepared easily and at low cost, preferably from compounds that are commercially available. The search for simple types of PR fluids has provided the motivation for our work in this area.

Recently, we have reported several types of simple PR fluids that can be prepared just by mixing two or three commercially available compounds. Thus, these fluids can be easily reproduced by other researchers who may lack skills in organic synthesis.[17,81]

Aqueous PR fluids that show either a viscosity decrease ("photothinning") or a viscosity increase ("photogelling") by irradiation with light have been reported, and these PR effects were based on changes in the size of micelles in water. In addition, our group has also recently reported a photothinning PR fluid based on nonpolar organic solvents.[82] Here, the decrease of viscosity relied upon changes in the sizes of reverse micelles formed by amphiphiles in these solvents. All of these simple PR fluids had a key limitation in that the viscosity changes were only one-way. Typically, the viscosity change was induced by ultraviolet (UV) light, but it could not be reversed by irradiation at alternate wavelengths.

In this paper, we will focus on the design of reversible PR fluids based on nonpolar solvents. As before, we would like to design these fluids with chemicals that can be purchased from commercial vendors rather than new materials that require synthesis in the laboratory. We begin with a system developed in our laboratory for the formation of reverse wormlike micelles (reverse worms), which are long, flexible cylindrical chains (Section 2.2). This is obtained by combining the phospholipid, lecithin, with bile salts such as sodium deoxycholate (SDC).[12-13] Lecithin/SDC reverse worms entangle and impart a high viscosity to many nonpolar solvents. To impart photoresponsive properties to these reverse worms, we have doped the micelles with a spiropyran derivative. Spiropyrans are well-known photochromic compounds (see Section 2.3), which can be reversibly photoisomerized between the colorless spiropyran (SP) form to the colored merocyanine (MC) form by irradiation at different wavelengths of light.[34-37] As shown in Figure 2.3, the closed SP form is hydrophobic and non-ionic

whereas the open MC form is zwitterionic and hydrophilic. The two forms of spiropyran are expected to interact differently with the headgroups of lecithin.[83-86] As we will show, they thus have different effects on the assembly of lecithin/SDC reverse worms. This leads to reversible light-induced changes in the rheological properties of the solutions.

4.2. EXPERIMENTAL SECTION

Materials. Soybean lecithin (95% purity) was purchased from Avanti Polar Lipids, Inc. The bile salt, sodium deoxycholate (SDC, >97% purity) was purchased from Sigma-Aldrich. The spiropyran, 1',3',3'-trimethyl-6-nitrospiro[1(2H)-benzopyran-2,2'-indoline] was obtained from TCI. Cyclohexane (> 99% purity) was from JT Baker.

Sample Preparation. Ground lecithin was dried in a vacuum oven at least for 48 h to remove residual water. Lecithin and SDC were mixed together in cyclohexane. The solutions became transparent and homogeneous by stirring and heating at 60°C. The sample was then cooled to room temperature and the spiropyran was added. The mixture was stirred till the spiropyran was completely dissolved.

Sample Response to Light. Samples were irradiated with UV light from an ORIEL 200 W mercury arc lamp. To access the UV wavelengths of the emitted light, a dichroic beam turner with a mirror reflectance range of 280-400 nm was used along with a < 400 nm filter. To nullify the effects of atmospheric moisture, the sample was contained in a capped quartz cell during UV irradiation. After UV irradiation, the colored dispersion was shaken and used for further studies. The sample was kept in a dark room to avoid

contact with visible light. A Varian Cary 50 UV-Vis spectrophotometer was used to monitor the color transition of the sample in response to UV. The sample for UV-Vis spectrophotometer was diluted four times compared to the original sample to avoid too high a value of the absorbance.

Rheology. Dynamic rheological experiments were performed on an ARES-G2 rheometer at the TA Instruments facility in Newark, DE. A high-pressure mercury lamp UV light source (150 mW/cm^2) having a 365 nm wavelength was fitted into the rheometer. This allowed real-time rheological measurements under UV irradiation, and subsequently in the absence of any irradiation. A parallel-plate geometry of 20 mm radius was used for all samples at ambient temperature. A solvent trap was used to minimize cyclohexane evaporation. Frequency spectra were conducted in the linear viscoelastic regime of the samples, as determined from dynamic strain sweep measurements.

4.3. RESULTS AND DISCUSSION

4.3.1 Rheology

The reversible PR fluids in our study are composed of lecithin, SDC, and spiropyran (SP) in cyclohexane. A typical composition of lecithin/SDC reverse worms consists of 100 mM lecithin and 35 mM SDC. At this concentration, the sample in cyclohexane is highly viscoelastic due to entangled reverse wormlike micelles. We added 15 mM of SP to this sample, which is about the maximum that can be dissolved in cyclohexane at ambient temperature. A photograph of the combined lecithin/SDC/SP sample is shown in the left panel of **Figure 4.1**. Note that the sample holds its weight in

the inverted vial, which is indicative of its viscoelastic character. Next, we subjected this sample to broad-band UV light. Within about 5 min, the sample became noticeably less viscous, and it also changed color from yellow to red. This is shown by the photograph in the middle panel of Figure 4.1, where the red liquid is seen to flow down the inverted vial. The change of color is typical for the conversion of SP (closed form) into MC (open form).[34-35] Thereafter, we switched off the UV light, and then within about 10 min, the sample recovered to its initial viscosity and color. This is shown by the photograph on the right panel of Figure 4.1 – note that the sample is back to holding its weight in the inverted vial. The recovery of the sample viscosity and color indicates the inverse conversion of MC into SP. These data are reproducible and the sample can be cycled more than 10 times without any deterioration of its response.

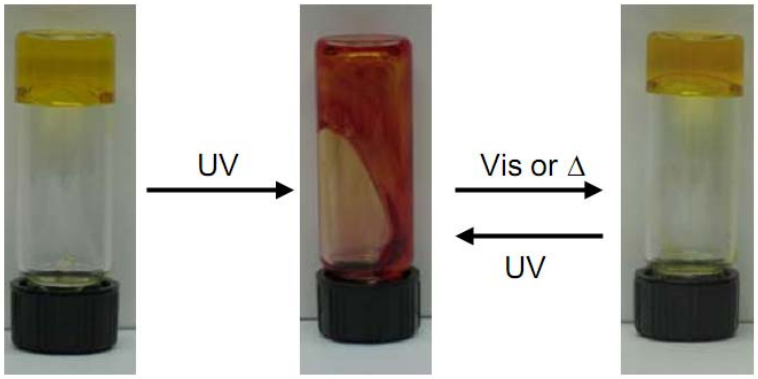

Figure 4.1. A sample of 100 mM lecithin + 35 mM SDC + 15 mM SP in cyclohexane (left). After UV irradiation, the viscosity of the sample drops and its color changes from yellow to red (middle). When the UV is stopped, the viscosity of the sample and its color increases back to its initial state (right). This cycle can be repeated several times.

We quantified the above rheological changes in real-time using a rheometer with a built-in UV apparatus. The sample was placed between transparent parallel plates and

irradiated with UV light at 365 nm and with an intensity of 150 mW/cm^2. The sample was monitored under oscillatory shear at a frequency of 7 rad/s. The results are plotted in **Figure 4.2** in terms of the complex viscosity η^*. Initially, the sample is viscous and its η^* is 2.5 Pa.s. When irradiated with UV light, the viscosity drops quickly and reaches a plateau value of about 0.2 Pa.s (10-fold) within about 100 s. At the 200 s mark, the UV is switched off, and at this point, the viscosity begins to grow back. It recovers to nearly its initial value in about 400 s.

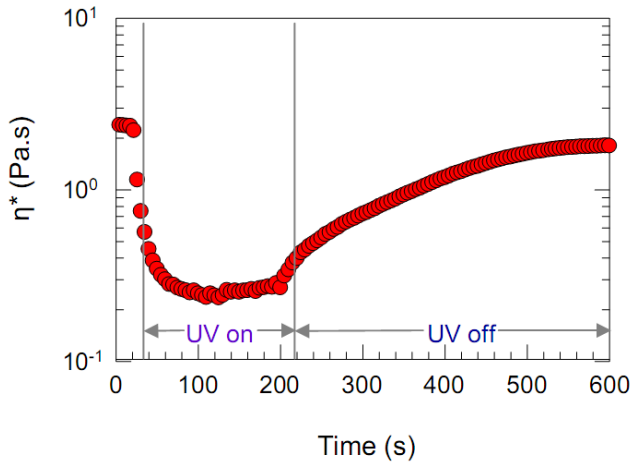

Figure 4.2. Real-time rheology of 100 mM Lecithin + 35 mM SDC + 15 mM SP sample in cyclohexane at ambient temperature. After 150 s of UV irradiation, the complex viscosity η^* of the sample decreases 10-fold. After switching off UV light at 200 s, the sample nearly recovers its full viscosity within about 400 s.

Figure 4.3 shows dynamic frequency spectra (elastic modulus G' and the viscous modulus G'' as functions of frequency ω) of the above sample. Initially, (**Figure 4.3a**), the data reveal a typical viscoelastic response. That is, at high ω or short timescales, the sample shows elastic behavior, with G' tending to a plateau and dominating over G''. On the other hand, at low ω or long timescales, the sample shows viscous behavior, with G''

exceeding G'. The longest relaxation time t_R of this viscoelastic sample can be estimated as $1/\omega_c$, where ω_c is the frequency at which G' and G'' cross, and it is initially ~ 80 ms. The value of the modulus at this frequency is about 195 Pa. We then ran the same frequency sweep under UV after the sample had been exposed to 180 s of UV. **Figure 4.3b** shows that the frequency spectra shift to higher frequencies, i.e., shorter timescales, as well as lower values of the moduli. Thus, the crossover of G' and G'' occur around 75 Pa, and the corresponding relaxation time is 13 ms. Finally, we switched off the UV and collected a frequency spectrum after 30 min, which was ample time to allow full recovery of the sample. **Figure 4.3c** shows that the spectra have reverted to close to their initial values. The crossover modulus in this case is about 180 Pa and the relaxation time is 40 ms. All in all, the sample is observed to become less viscoelastic upon irradiation with UV, while it recovers its initial viscoelasticity after the UV is switched off. The decrease in viscoelasticity suggests a UV-induced shortening of the reverse worms, allowing the worms to become less entangled and relax faster. When the UV is switched off, the worms appear to regain their initial length.

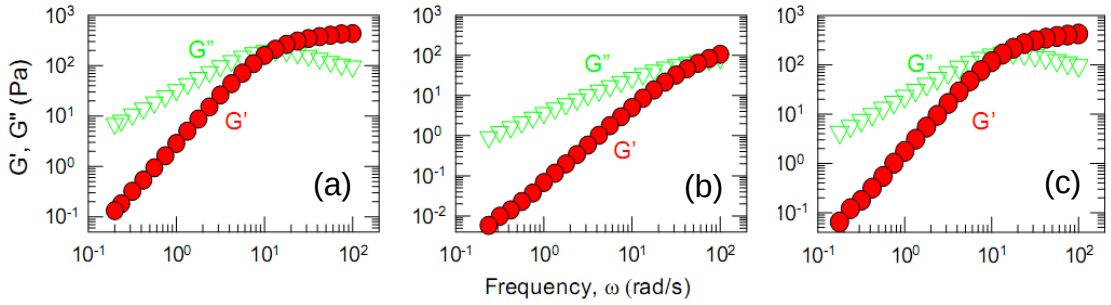

Figure 4.3. Dynamic rheology of a 100 mM Lecithin + 35 mM SDC + 15 mM SP sample in cyclohexane: (a) before UV irradiation, (b) during UV irradiation, and (c) 30 min after switching off the UV. Each plot shows the elastic modulus G' and the viscous modulus G'' as functions of frequency ω.

4.3.2. UV-Vis Spectroscopy

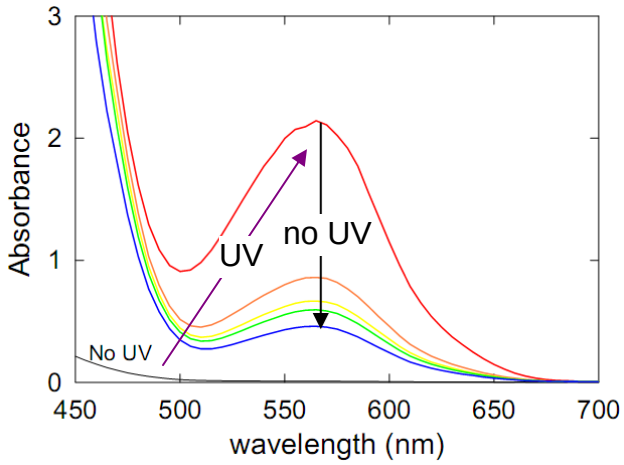

Figure 4.4. UV-vis spectra of a 25 mM lecithin + 8.75 mM SDC + 3.75 mM SP sample in cyclohexane. A peak at 565 nm develops upon UV irradiation, indicating the conversion of SP to MC. The UV is then switched off and spectra are gathered after different wait times (0, 2, 6, 10 and 20 min from the top). The peak is observed to decrease, indicating the reversion of the MC to SP.

UV-Vis spectra (**Figure 4.4**) confirm that the rheological changes are accompanied by the photoconversion of SP to MC and back. We used a diluted sample (25 mM lecithin + 8.75 mM SDC + 3.75 mM SP) to ensure the proper levels of absorbance. The initial sample has a weak absorbance in the range of wavelengths shown, which correlates with the colorless nature of the SP form. When irradiated with UV light for 3 min, the sample transforms to a red liquid, and correspondingly, a strong absorption peak arises at 565 nm. This indicates the UV-induced conversion of the closed SP form into the open MC form. The UV is then switched off and we collect spectra after different wait times. We note that the peak at 565 nm decreases as time goes on, and the sample correspondingly shows a transition in color from red to yellow. This occurs because the MC in nonpolar solvents is often thermally unstable, and thus it reverts to the SP form

even in the dark.[34-35] In short, the peak increase under UV indicates SP to MC conversion, while the peak decrease after UV is switched off indicates a reversion from MC to SP.

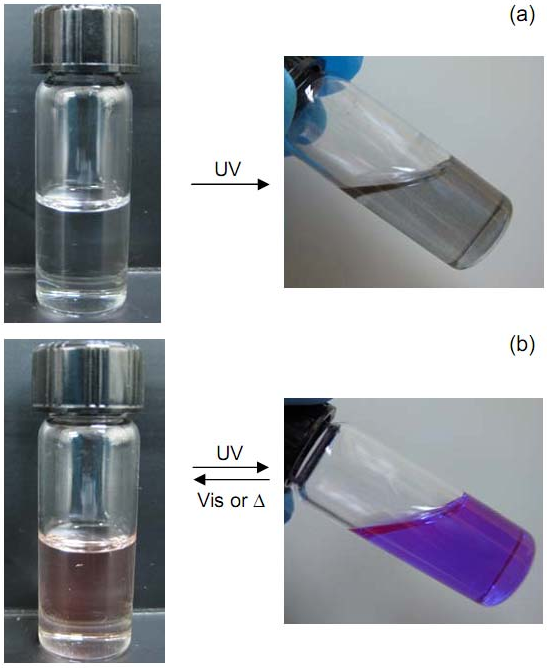

Figure 4.5. (a) 5 mM SP is solubilized in cyclohexane (left), but after UV irradiation, the MC precipitates out due to its polarity (right). (b) 3.75 mM SP solubilized in a 25 mM lecithin organosol in cyclohexane (left). After UV irradiation, the sample color changes to purple and it shows no precipitation (right). This indicates the binding of MC to lecithin headgroups (right).

4.3.3. Mechanism

We now wish to understand why the viscosity of lecithin/SDC decreases when the SP is converted to MC. In this context, we note that the SP form is quite soluble in non-polar solvents, whereas the MC form is relatively insoluble due to its hydrophilic nature. This is shown by **Figure 4.5a**: first, we show that 5 mM of SP gets solubilized in neat cyclohexane. However, when irradiated with UV, the SP converts to MC, and the latter precipitates out of the cyclohexane. Next, in **Figure 4.5b**, we show a variation of the

same experiment for the case where lecithin is present in the cyclohexane. Once again, the SP is solubilized in the lecithin organosol. But in this case, when irradiated with UV, the solution remains homogeneous and takes on a violet-red color. The homogeneity shows that the MC form must be solubilized within lecithin micelles. Due to its hydrophilic and zwitterionic nature, it is likely that the MC binds to the zwitterionic phosphocholine head groups of lecithin.

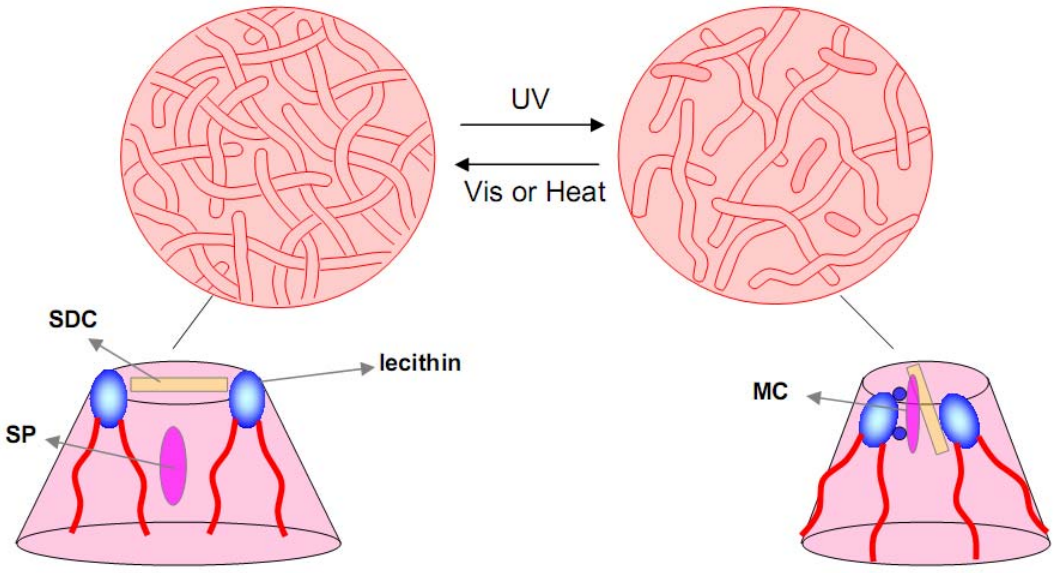

Figure 4.6. Mechanism of action in the case of lecithin/SDC/SP-based PR fluids. The mechanism relies on distinct effects of the SP and MC photoisomers on reverse self-assembly. Before UV irradiation (left), the SP remains in the hydrophobic area, surrounded either by the solvent or the hydrophobic tails of lecithin. The net molecular geometry is that of a truncated cone, which favors growth of micelles. Upon UV irradiation, the SP converts to MC, which shifts to the headgroup area of lecithin due to its hydrophilicity. The size of headgroup area reduces resulting in a molecular geometry closer to a cone. In turn, the assemblies transform into shorter cylindrical micelles, which are less entangled and relax faster.

We therefore suggest a tentative mechanism to explain the different interactions of SP and MC with lecithin/SDC reverse worms, and this is shown in **Figure 4.6**. First, when SP is added to lecithin-SDC mixtures, it will probably reside in the non-polar

solvent or next to the tails of lecithin. Note that lecithin and SDC are expected to interact via hydrogen-bonding between the hydroxyls of SDC and the headgroups of lecithin. It is due to such interactions that the net geometry of the amphiphile favors growth of reverse worms. Due to its nonpolar nature, the SP has relatively no effect on lecithin-SDC interactions. Next, when SP is converted to MC, the zwitterionic MC is likely to bind to lecithin headgroups, displacing some of the SDC in the process. In the process, the net geometry seems to get altered in a way that disfavors growth of worms – i.e., it induces the micelles to shorten. The shorter worms evidently entangle less and relax faster, which can explain the reduction in viscosity.

4.4. CONCLUSIONS

In conclusion, we have presented a PR system in which reversible viscosity changes can be induced by light. The system is based on mixtures of lecithin, the bile salt, SDC, and a spiropyran – notably all these components are commercially available. The viscosity of the solution decreases 10-fold when UV is switched on, and recovers its initial value when UV is switched off. Also, this cycle can be repeated more than 10 times without deterioration in the response. We suggest that these results are caused by the differential interaction of the zwitterionic lipid, lecithin with the SP and MC forms of the spiropyran.

Chapter 5

REVERSE MULTILAMELLAR VESICLES IN MIXTURES OF LIPIDS AND MULTIVALENT CATIONS

5.1. INTRODUCTION

In this chapter, we describe a new route for the formation of reverse bilayer structures such as reverse vesicles and lamellar sheets in nonpolar solvents. Reverse vesicles are structures that contain oil in the core and covered by a reverse bilayer shell or shells. The reverse bilayer consists of amphiphiles whose hydrophobic tails are exposed to the oil both in the core and in the exterior, while the hydrophilic headgroups are shielded from the oil. Reverse vesicles have the possibility to be used for encapsulation and controlled delivery of diverse molecules in the same way as normal vesicles.[21] However, there are only a few scattered reports of reverse vesicles in the literature, many of which have relied on exotic amphiphiles.[20-22,24-27,33] Recently, we showed a new simpler route to reverse unilamellar vesicles by combining short- and long-chain lecithins. The geometry of the reverse aggregates could be tuned from reverse spheres to reverse cylinders to reverse vesicles by controlling the molar ratio of the two lecithins.

The class of systems reported here has similarities to those described in Chapter 3. In that case, we combined the unsaturated phospholipid, lecithin with salts of multivalent cations to produce reverse cylinders.[87] Here, we add similar salts to a *saturated* phospholipid within a nonpolar solvent. The main lipid of interest is 1,2-dimyristoyl-*sn*-

glycero-3-phophocholine (DMPC), and the multivalent cations we will focus on are calcium (Ca^{2+}) and gadolinium (Gd^{3+}). DMPC has two saturated C_{14} tails, which give it a high melting temperature and make it also insoluble in oils such as cyclohexane at room temperature. However, even though both salts and DMPC are individually insoluble in oil, when the two are mixed together, their mixtures are able to dissolve at certain molar concentration to form homogeneous and single-phase solutions. Surprisingly, such solutions are quite stable without precipitation for several weeks.

Because DMPC has the same headgroup as lecithin, we can expect an ionic interaction between DMPC and multivalent cations much like that described in Chapter 3. Thus, we would expect DMPC-cation mixtures to form reverse cylindrical micelles and give rise to gels. However, the surprising finding is that these mixtures show a further transition with increasing salt from reverse cylinders to reverse vesicles/lamellae. No such structures were noted in the case of lecithin-cation mixtures. The difference might arise because the tails of DMPC are saturated, which allows their tighter packing. We will discuss this mechanism in detail later. Another notable point arises from the use of Gd^{3+}, which is an ion that finds application as a contrast agent in magnetic resonance imaging (MRI). Thus, it is possible that reverse vesicles formed in DMPC-salt mixtures might be useful in a vareity of applications, including as a delivery or contrast agent.

5.2. EXPERIMENTAL SECTION

Materials. The saturated phospholipid, 1,2-dimyristoyl-*sn*-glycero-3-phophocholine (DMPC, C_{14}) in chloroform was purchased from Avanti Polar Lipids, Inc. Other saturated

phospholipids, 1,2-dilauroyl-*sn*-glycero-3-phosphocholine (DLPC, C_{12}), 1,2-dipalmitoyl-*sn*-glycero-3-phosphocholine (DPPC, C_{16}) and 1,2-distearoyl-*sn*-glycero-3-phosphocholine (DSPC, C_{18}) were purchased from NOF Corp. (Tokyo, Japan). Anhydrous (>99.99% purity) NaCl, $CaCl_2$ and $GdCl_3$ were purchased from Sigma-Aldrich. Cyclohexane (> 99% purity) was from JT Baker.

Sample Preparation. Mixed solutions containing lipid and salt were prepared as follows. Salts were dissolved in methanol to form 100 mM stock solution. Desired compositions of the samples were achieved by mixing the lipid in chloroform and the salt stock solutions. The solvent was removed by drying the samples under a fume hood for 24 h and then in a lyophilizer connected a vacuum pump for at least 48 h. The final samples were prepared by adding the nonpolar solvent like cyclohexane, followed by stirring and heating at around 60°C until the solutions became homogeneous and transparent. The above procedure ensured the removal of any residual water from the sample, and thereby facilitated reproducible sample preparation. The samples were equilibrated for 1 day at room temperature prior to conducting experiments.

Dynamic Light Scattering (DLS). A Photocor-FC light scattering instrument with a 5 mW laser light source at 633 nm was used at 25 °C, with the scattering angle being 90°. A logarithmic correlator was used to collect the autocorrelation function, from which a diffusion coefficient was obtained. The hydrodynamic size was calculated from the diffusion coefficient through the Stokes-Einstein relationship (eq 2.10).

Transmission Electron Microscopy (TEM). TEM was conducted on a Jeol JEM 2100 microscope at 100 KeV. A carbon-coated copper grid was dipped into the solution for 10 s without any staining and the solution on the grid was carefully thinned by blotting with a soft paper. The grid was then dried in a fume hood for 24 h before imaging.

Rheology. Dynamic rheological experiments were performed on an AR2000 stress controlled rheometer (TA Instruments). Cone-and plate geometry of 20 mm diameter/2° cone-angle was used. The plates were equipped with Peltier-based temperature control and all samples were studied at 25°C. A solvent trap was used to minimize cyclohexane evaporation. Dynamic frequency spectra were conducted in the linear viscoelastic regime of the samples, as determined from dynamic strain sweep measurements.

Small Angle X-ray Scattering (SAXS). SAXS measurements were done on a Nano-STAR instrument (Bruker AXS Inc.) with a CuK radiation source operating at 45 kV/120 mA. The distance between the sample and the counter was 1060 mm, allowing the value of the scattering vector q to range from 0.15 to 3.0 nm^{-1}. The sample was injected into a 2 mm-diameter glass capillary. All measurements were performed at 25°C.

Differential Scanning Calorimetry (DSC). The phase transition temperatures of lipids in solution were measured on a Rigaku DSC-8230 at the rate of 2°C/min. The temperature scanning range was 0-70°C and the N_2 flow rate was 50 mL/min. The empty vessel was used as a reference. The sample (15 mg) was put in a stainless steel pan with a resistance pressure of 50 atm and the vessel was sealed to prevent sample evaporation.

5.3. RESULTS AND DISCUSSION

5.3.1. Phase Behavior

Figure 5.1. Photographs of mixtures of DMPC (18.5 mM) with varying concentrations of Gd^{3+}. At 2 mM Gd^{3+}, the sample precipitates out. At 7 mM Gd^{3+}, the sample is gel-like, indicating cylindrical micelles. At 12 mM Gd^{3+}, the sample is non-viscous and has a slight bluish color, indicating the onset of reverse vesicles. At 16 mM Gd^{3+}, the sample is much more turbid, indicating the presence of substantial reverse vesicles.

We first show results for mixtures of DMPC and anhydrous gadolinium chloride ($GdCl_3$) in cyclohexane. DMPC does not dissolve in cyclohexane at room temperature and forms a solid precipitate due to its melting temperature being around 34°C. In addition, $GdCl_3$ does not dissolve in cyclohexane either. However, when mixed at certain molar ratios, both components dissolve and become homogeneous in cyclohexane at room temperature. **Figure 5.1** shows mixtures of 18.5 mM DMPC with varying [Gd^{3+}]. For 4 mM Gd^{3+} or lower, precipitation occurs. At slightly higher Gd^{3+}, the sample becomes homogeneous and transparent, and its viscosity begins to increase. Samples with about 7-8 mM Gd^{3+} are transparent gels, and they hold their weight in the inverted vial.

Dynamic rheological data (**Figure 5.2**) confirms the gel-like nature. Here, the elastic G' and viscous G'' moduli are found to be nearly independent of frequency ω, with G' exceeding G'' across the frequency range. This result is quite similar to that obtained for mixtures of unsaturated lecithin with multivalent ions (Chapter 3). As in that case, we attribute the gel-like behavior to the entanglement of long cylindrical reverse micelles.

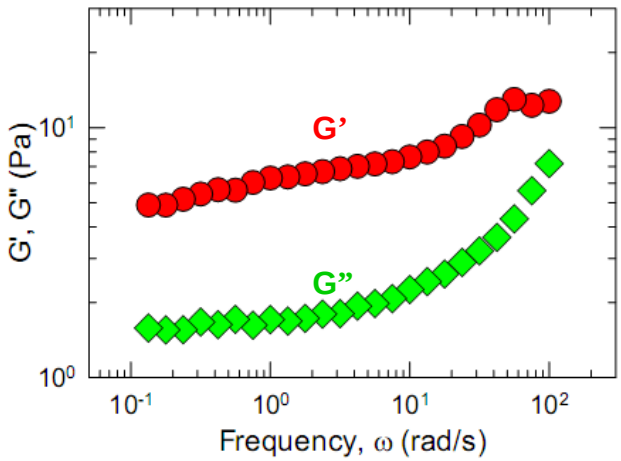

Figure 5.2. Dynamic frequency spectra (elastic modulus G' and viscous modulus G'' moduli as functions of frequency ω) for a gel-like sample of 18.5 mM DMPC and 7 mM Gd^{3+} in cyclohexane at 25°C.

Beyond about 9 mM, further increase in [Gd^{3+}] caused the viscosity of the samples to rapidly decrease. By about 12 mM Gd^{3+}, the viscosity became essentially identical to that of the solvent. A slight bluish tinge could be observed for the 12 mM sample, as shown in Figure 5.1. This bluish tinge intensified as the [Gd^{3+}] was increased further. At a [Gd^{3+}] of 16 mM, the sample was quite turbid, as seen also in Figure 5.1. In the latter case, a slight precipitation was observed with time. However, samples in the range of 12-14 mM remained homogenous and bluish for several weeks.

The above results provide preliminary evidence for a phase transition from reverse cylinders to reverse vesicles with increasing [Gd^{3+}]. Analysis of the 12 mM Gd^{3+} sample by DLS gave an average hydrodynamic diameter d_h of 82 nm for the structures in this solution. The corresponding values of d_h were 140 nm for the 14 mM Gd^{3+} sample and 440 nm for the 16 mM Gd^{3+} sample.

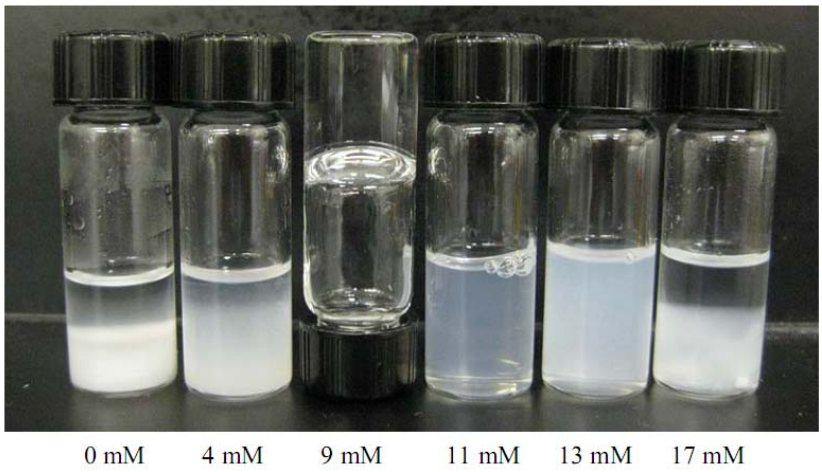

Figure 5.3. Photographs of mixtures of DMPC (20 mM) with varying concentrations of Ca^{2+}. At 0 and 4 mM Ca^{2+}], the sample precipitates out. At 9 mM Ca^{2+}, the sample is gel-like, indicating cylindrical micelles. At 11 mM Ca^{2+}, the sample is slightly viscous and has a slight bluish color. At 13 mM Ca^{2+}, the sample is bluish with the same viscosity as the solvent. At 17 mM Ca^{2+}, the sample separates into two phases.

The above pattern of phase behavior was also observed with other divalent or trivalent cations. **Figure 5.3** illustrates the behavior for mixtures of DMPC (20 mM) with anhydrous $CaCl_2$. The results for increasing [Ca^{2+}] are similar to those for [Gd^{3+}] in Figure 5.2: from precipitate to transparent gels to low-viscosity bluish solutions to more turbid solutions. Thus, in the range of 12-14 mM Ca^{2+}, we again see visual evidence for

reverse vesicles. We also tested monovalent salts like NaCl; however, mixtures of DMPC and NaCl formed a precipitate at all concentrations tested.

In addition to DMPC, we also examined several other saturated phospholipids, including those with shorter tails like DLPC (C_{12}), as well as those with longer tails like DPPC (C_{16}) and DSPC (C_{18}). DPPC and DSPC have higher melting temperatures than DMPC, and in these cases, the addition of multivalent cations was not sufficient to solubilize them at room temperature in cyclohexane. In the case of DLPC, mixtures with multivalent cations formed transparent gels at certain molar ratios, but the reverse vesicle region with the non-viscous bluish solutions was not observed.

5.3.2. Nanostructure from TEM

TEM micrographs of samples with 18.5 mM DMPC and 12 mM Gd^{3+} are shown in **Figure 5.4** in the absence of any staining. The images show a number of spherical structures with multiple concentric bilayer shells, which are indicative of multilamellar reverse vesicles ("onions"). The outlines of three such vesicles are shown in the top image. The bottom image is a close-up showing the bilayers around a couple of vesicles. Note that the Gd^{3+} in the vesicles (bound to the lipid headgroups) acts as an intrinsic contrast agent, allowing the bilayers to be seen clearly under TEM. The reverse vesicles have a diameter around 100-120 nm and there appear to be 5-7 concentric bilayers around each vesicle. For any given vesicle, some portions of the strucutre are not visible, i.e., the vesicles appear to be incomplete. This may be an artifact caused by a partial collapse of the bilayers when the sample is dried on the TEM grid.

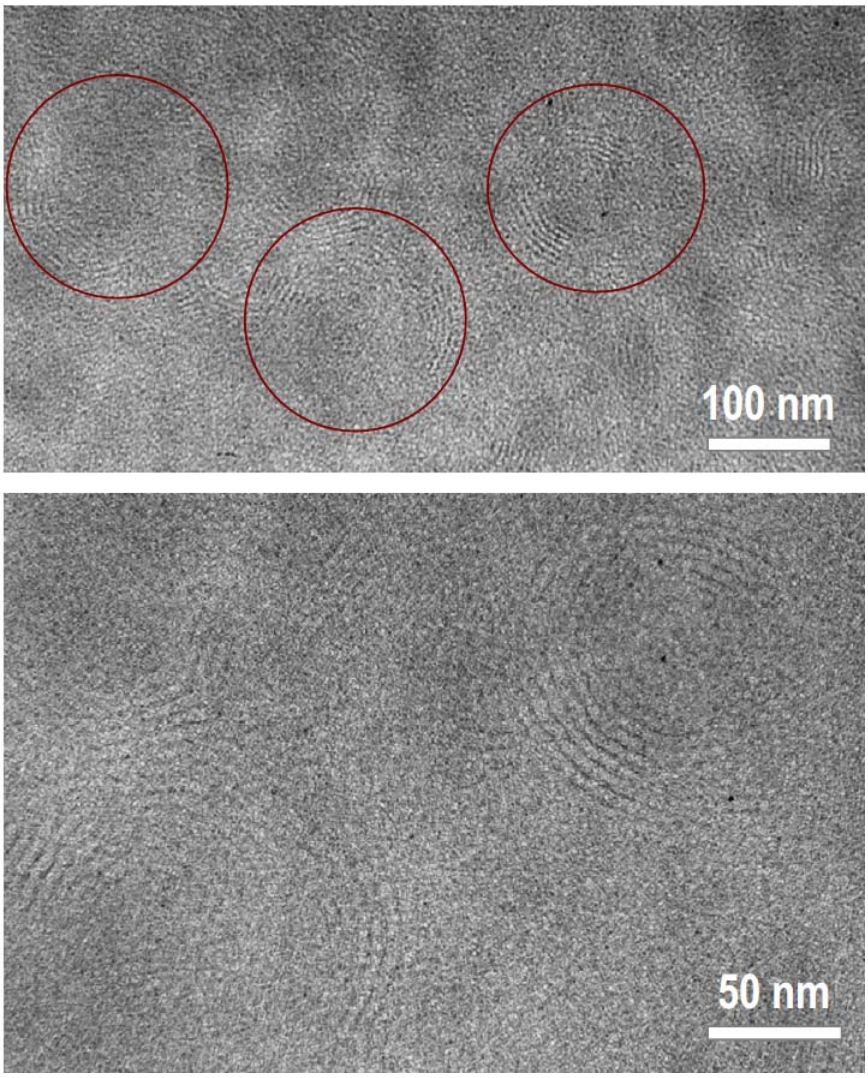

Figure 5.4. TEM images of structures present in a sample of 18.5 mM DMPC + 12 mM Gd^{3+} in cyclohexane. Multilamellar reverse vesicles (circled) are visible in these images. The bottom image shows a close-up of the concentric bilayers surrounding a couple of the vesicles.

TEM images were also acquired on a sample containing 18.5 mM DMPC and 16 mM Gd^{3+}, again without additional staining. Recall that this sample exhibited a higher size under DLS and it also showed a stronger turbidity along with a slight precipitation. Under TEM (**Figure 5.5**), this sample revealed a few partially ruptured multilamellar

vesicles (blue arrow) as well as numerous stacks of lamellar fragments (red arrows). Similar images have been observed for lamellar phases in water.[88] Thus, the TEM images suggest a progression from reverse multilamellar vesicles to reverse lamellae with increasing [Gd^{3+}].

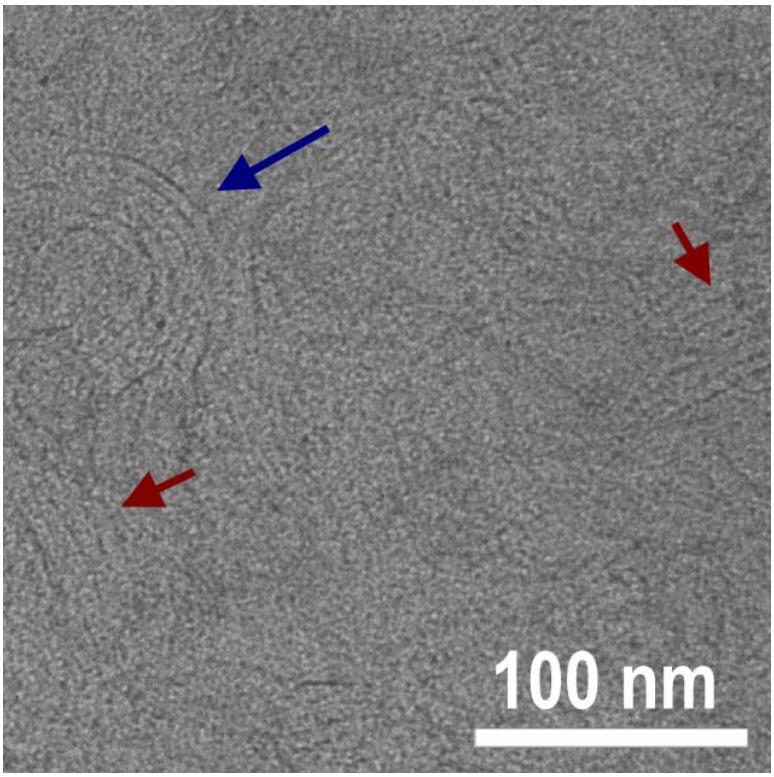

Figure 5.4. TEM image of structures present in a sample of 18.5 mM DMPC + 16 mM Gd^{3+} in cyclohexane. Fragments of multilamellar reverse vesicles (blue arrow) as well as lamellar stacks (red arrows) are seen in the image.

5.3.3. Nanostructure from SAXS

To further clarify the microstructures in these samples, we made use of SAXS. SAXS spectra (intensity *I* vs. scattering vector *q*) for 18.5 mM DMPC with three different concentrations (7, 12 and 16 mM) of Gd^{3+} are shown in **Figure 5.6**. The 7 mM Gd^{3+}

sample shows a q^{-1} decay of the intensity at low q, which essentially corresponds to cylindrical structures. The gel-like nature of this sample can be reasonably explained by the entanglement of these cylindrical structures. In the case of the sample with 12 mM Gd^{3+}, the data shows a q^{-2} decay of the intensity at low q, which reflects the presence of bilayer structures. This correlates nicely with the presence of reverse vesicles in the TEM images of the same sample. Finally, the sample with 17 mM Gd^{3+} shows a sharp peak at a relatively high q value of 1.05 nm^{-1}. This type of plot is indicative of lamellar structures, which is also in good agreement with the TEM image of the sample. From the peak position q_0, the inter-bilayer spacing $d = 2\pi/q_0$ is determined to be 6.0 nm.

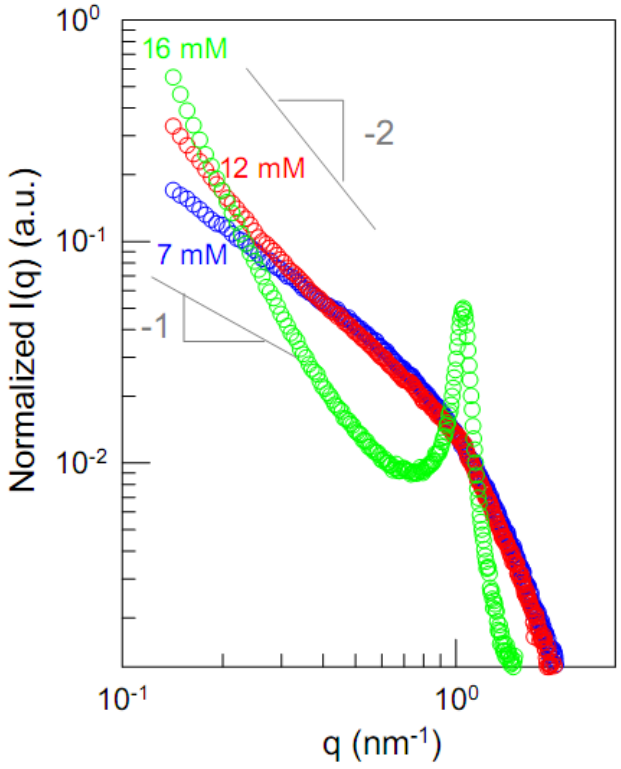

Figure 5.6. SAXS data at 25°C from mixtures of DMPC and Gd^{3+} in cyclohexane. The samples each contain 18.5 mM DMPC while the Gd^{3+} concentrations were 7 mM, 12 mM and 16 mM.

5.3.4. Thermal Response from DSC

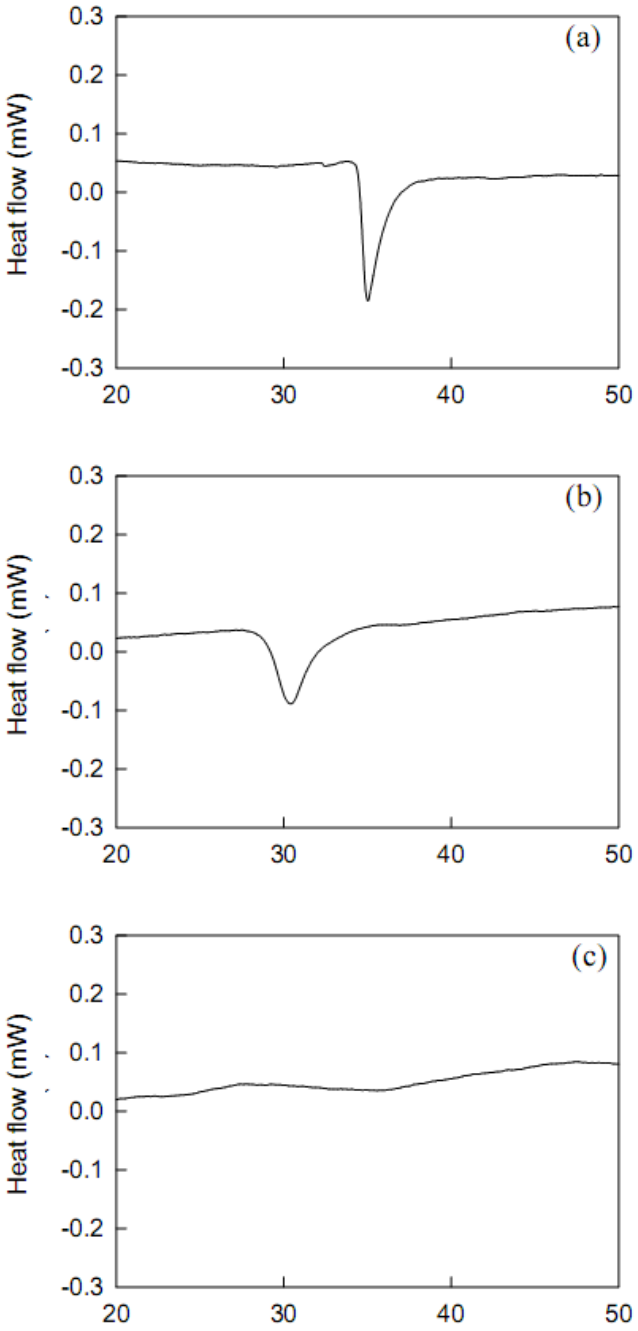

Figure 5.7. DSC for samples of 18.5 mM DMPC + (a) 0 mM, (b) 4 mM and (c) 7 mM Gd^{3+} in cylcohexane. The 0 mM and 4 mM samples show peaks at 34.4°C and 28.7 °C respectively, which originates from the melting temperature of DMPC. In case of the 7 mM sample, this peak is absent, indicating the increase of DMPC solubility.

DSC was used to probe the melting transitions of DMPC at 18.5 mM in cyclohexane with different [Gd^{3+}] added. Below the melting temperature T_m, the alkyl tails in DMPC are said to be in a "frozen" state, whereas above T_m, the tails are liquid-like and flexible. T_m is generally of great relevance to bilayers of DMPC in water, i.e., below T_m, the bilayers are in a "gel" phase whereas above T_m, the bilayers are in a liquid-crystalline phase. Experimental values of T_m for DMPC bilayers in water are around 23°C.[89] Here, DMPC is being probed in a nonpolar organic liquid. The sample of DMPC alone in cyclohexane (**Figure 5.7a**) does show an endothermic peak at 34.4°C. As mentioned earlier, we attribute the low solubility of pure DMPC in cyclohexane to this high T_m, i.e., to the fact that the chains are ordered and rigid.

Next, we note the DSC curve for the cases when Gd^{3+} is added to the DMPC sample. For 4 mM Gd^{3+} (**Figure 5.7b**), the endothermic peak shifts down to 28.7°C. When the Gd^{3+} is further raised to 7 mM (**Figure 5.7c**), the peak vanishes. This shows that the addition of Gd^{3+} reduces and then eliminates the melting peak due to DMPC. The lack of a peak at 7 mM Gd^{3+} implies that the melting temperature is too low to be measured (note that cyclohexane freezes around 6.7°C, which poses a necessary limitation in the DSC experiment). From these data, we can conclude that there is a strong interaction between Gd^{3+} and DMPC, one effect of which is to liquefy the tails of DMPC. These data help to explain why mixtures of DMPC/Gd^{3+} in cyclohexane are soluble and homogeneous even though the individual components are each insoluble in the same solvent.

5.3.5. Mechanism

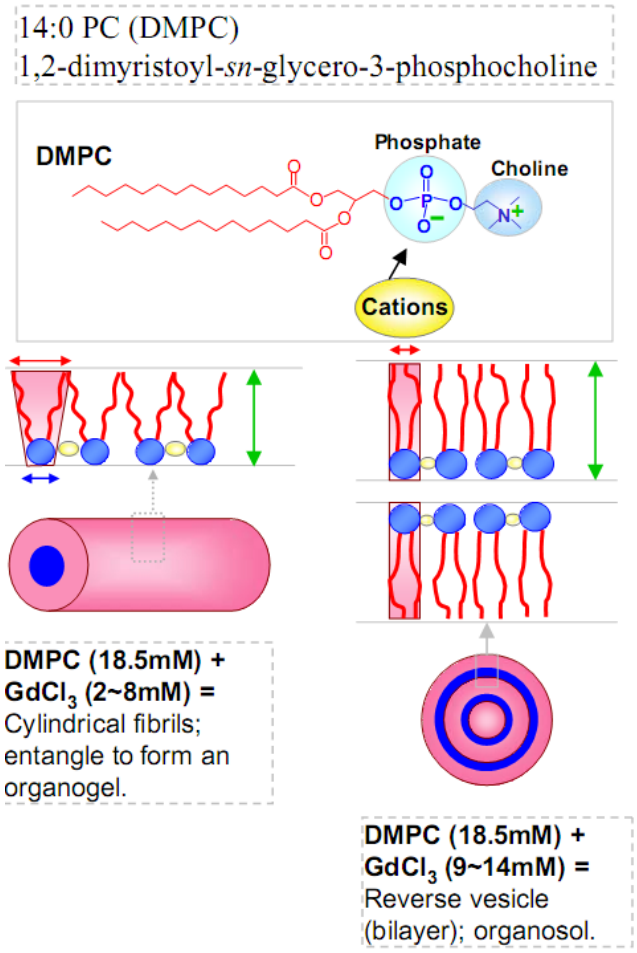

Figure 5.8. The effects of cations, such as $GdCl_3$, on assembly of DMPC in cyclohexane are shown. The top panel shows the structure of DMPC, which features two saturated carbon tails and a polar phosphocholine headgroup. The bottom left panel ($GdCl_3$< 8 mM) demonstrates Gd^{3+} ions (yellow spheres) binding to DMPC, which induces an increase in the headgroup area a_{hg} (blue arrow). The tails straighten and become more rigid, which causes the tail area a_{tail} to decrease (red arrow). The molecular geometry takes the shape of a truncated cone, which allows the lipids to pack in cylindrical fibrils. These fibrils entangle to increase sample viscosity. The bottom right panel ($GdCl_3$ 9-14 mM) shows further stiffening of the DMPC tails as more Gd^{3+} ions are added. The molecular geometry of the lipids takes on a cylindrical shape. These cylinders are thus able to pack tightly into bilayers, which result in the formation of reverse vesicles.

We will now discuss the mechanism by which multivalent cations induce DMPC to assemble into a variety of reverse self-assembled structures. Interactions between

cations and phospholipids in water have been well-studied, both by experiments and by simulations. In general, cations have tendency to bind to the polar headgroup of phospholipids, and multivalent cations can bind to more than one cation at the same time. Such binding of the cations forces the phospholipid tails to be more densely packed and thus in a more extended configuration, as was explained in Chapter 3. In turn, this causes a decrease of the average cross-sectional area a_{tail} of the lipid.

In Chapter 3, we had discussed the binding of multivalent cations with the phosphocholine headgroups of lecithin, which then induces a transition from reverse spherical micelles to reverse cylindrical structures. On the molecular level, we attributed the effect of cation-binding to be either to expand the headgroup area (a_{hg}) or to decrease the tail area (a_{tail}) due to the straightening of lipid tails (**Figure 5.8**). The same arguments still hold in the case of DMPC, which has the same headgroups as lecithin. The difference with DMPC is that a further transition occurs from reverse cylinders to reverse bilayers (vesicles), which did not occur in the case of lecithin. We believe the explanation for the latter transition lies in the saturated tails of DMPC. Since both tails of DMPC are saturated, compared to the unsaturation in one tail of lecithin, the tails by themselves are more flexible, and such tails may be able to straighten more when cations bind with DMPC. In other words, the geometrical transformation of DMPC can be more pronounced due to its flexible tails.

The geometry argument can be explained in terms of the critical packing parameter $p = a_{tail}/a_{hg}$, where a_{tail} and a_{hg} are the cross-sectional areas of amphiphile's tail

and headgroup, respectively. In the case of organic solvents, the formation of reverse spherical micelles requires a packing parameter p much larger than 1, implying an inverse cone shape. When the packing parameter p decreases through either an expansion of the headroup area a_{hg} or a shrinking of the tail area a_{tail}, the formation of reverse cylinders or bilayer structures is induced by transformation of lipid geometry into a truncated cone shape or a cylinder shape. Accordingly, ion binding may cause a decrease in p as depicted in **Figure 5.8.**

5.4. CONCLUSIONS

This study has demonstrated that multivalent cations such as Ca^{2+} and Gd^{3+} can affect the self-assembly of saturated phospholipids like DMPC in organic solvents. The cations are expected to bind to the headgroups of the lipid, and they may also affect the orientation of the lipid tails. At low concentrations, the cations induce reverse cylindrical micelles, which in turn entangle to produce gel-like samples. At higher concentrations, the cations induce reverse multilamellar vesicles (onions) with an overall size of around 100 nm and with several concentric shells. At even higher concentrations of the cations, a phase consisting of reverse lamellae is produced. Reverse onions and reverse lamellae are very unusual structures, and our study shows how these can be readily assembled in nonpolar solvents. Future studies will determine if these structures are potentially useful as controlled release vehicles or as contrast agents in imaging studies.

Chapter 6

CONCLUSIONS AND RECOMMENDATIONS

6.1. CONCLUSIONS

Self-assembly using amphiphilic molecules in nonpolar solvents has been less-known compared to that in aqueous system. Previous studies about reverse self-assembly have focused upon lecithin in conjunction with other additives such as water and bile salts. Such combination can alter molecular geometry of lecithin and, in turn, aggregate morphology is also changed. In this dissertation, we have reported new reverse self-assembly by combination of lecithin and more common, inorganic salts. In addition to this, we have also developed a new simple route to create reversible photorheological (PR) fluids by doping lecithin/bile salt reverse worms with spiropyran. All materials that have been used for these systems are commercially available and any difficult synthesis has not been used to prepare the samples.

We have shown that the addition of multivalent cations to lecithin organosols can induce a transition from organosols containing spherical micelles to organogels containing cylindrical micelles (Chapter 3). Interestingly, inorganic salts such as $CaCl_2$ can be dissolved in nonpolar solvents in the presence of lecithin and bind with the headgroups of lecithin by electrostatic interactions just like in water. The binding of lecithin with cations can alter the effective geometry of lecithin to that of a truncated cone inducing cylindrical structures. The organogel can support its own weight in a

overturned vial since the network that includes fibrils can hold solvent through capillarity. Also, the gel can be broken easily with a small amount of polar solvent such as ethanol.

In addition to organogels formed by networks of fibrils, we have studied about PR fluids using reverse worms doped with spiropyran (Chapter 4). Reverse worms that have viscoelastic properties are prepared by the mixture of lecithin/SDC and the spirypyran is added to create such PR fluids. Spiropyrans are well-known photochromic compounds that induce reversible isomerization between closed-spirypyran (SP) form and open-merocyanine (MC) form by UV (SP to MC) or visible light (MC to SP) irradiation. Upon UV irradiation, the viscosity of the sample decreases up to 10-fold of the initial viscosity. Reversely, the viscosity of the sample recovers to the initial viscosity of the sample after switching off the UV. The materials such as lecithin, SDC and spiropyran that are used to make reversible PR fluids are cheap and commercially available, and, unlike other reversible PR fluids in nonpolar liquids, special and difficult synthesis are not required to prepare the sample.

In Chapter 5, we have extended Chapter 3 studies to saturated phospholipids such as DMPC. The tails of the saturated lipids are more flexible than those of the unsaturated lipids since double or triple bonds that enhance the rigidity of the tails do not exist in the hydrocarbon tails. Accordingly, when cations bind with the headgroups of a saturated lipid, the tails of a saturated lipid can be more straightened than those of an unsaturated lipid inducing the reduction of tails area. This can make the effective molecular geometry cylindrical shape and, in turn, reverse bilayer like vesicles may be formed.

6.2. Recommendations for Future Work

Based on the systems we have reported, it is highly possible to explore new reverse systems following the hypotheses and ideas we have provided. Moreover, although this dissertation focuses on the fundamental aspect of reverse self-assembly, the applications of these new systems may be promising. We suggest three feasible projects for the future work briefly described as below:

6.2.1. Reverse Aggregates Induced by Anions

The hypothesis of formation of reverse worms in Chapter 3 was that the addition of metal ions such as multivalent cations alters the net geometry of lecithin from one that favors spheres to one favoring cylinders. In Chapter 3, we mainly focused on the effect of multivalent cations which are able to bind with lecithin so that they can alter the effective

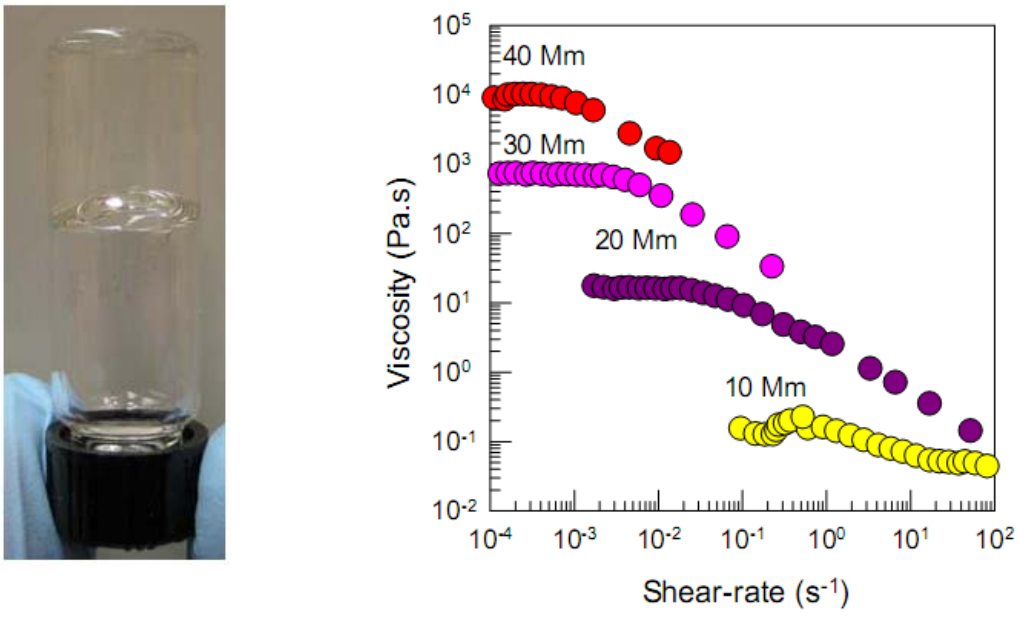

Figure 6.1. Photograph of a sample containing 40 mM lecithin and 40 mM NaBr in decane. The sample supports its own weight in the overturned vial (left). Viscosity vs. shear-rate plots are shown for a 40 mM lecithin/40, 30, 20 and 10 mM NaBr in decane (right).

geometry. In fact, most of the studies in aqueous system have also focused on the cations with phospholipids. However, in aqueous system, a few studies have been shown that anions as well as cations can bind with zwitterionic phosphocholine headgroups[90] even though the effect of anions on the phospholipids is still controversial. Since, lecithin is well-known as a zwitterion, we expect that anions can also bind with phosphocholine headgroups. As mentioned above, lipid-ion mixtures in oil are analogous in many ways to the same mixtures in water. In fact, our experiments have shown that while NaCl does not induce the gel formation with lecithin, the mixture of NaBr/lecithin can form organogel (**Figure 6.1 (a)**). Steady rheology of lecithin/NaBr **(Figure 6.1 (b))** shows the increase of the sample viscosity as NaBr concentrations increase. This result is very similar to that of lecithin/cations. Based upon the result, we again conjecture that this effect is due to the binding of Br^- to lecithin headgroups and the resulting alteration of the molecular geometry. As part of future work, the effects of different types of anions and their concentration on reverse self-assembly can be systematically studied.

In addition to the effect of anions on lecithin, the potency of lipid-ion gelators could be further improved by finding rational choice of the lipids. For example, ionic lipids like phosphatidylglycerols (PG) and phosphatidylserines (PS) are known to bind with cations compared to the zwiterrionic phosphatidylcholineS (PC). Also, lipids in gel (frozen) state can have stronger binding affinity with ions than that in liquid crystalline state. Thus, an anionic lipid with long unsaturated tails, when combined with cations, might be a very potent organogelator.

6.2.2. Development of Reversible PR Fluids

The results of Chapter 4 demonstrate that a reversible PR fluid that has 10-fold change in η^* can be realized in nonpolar solvents using simple, commercially available components such as lecithin, SDC and spiropyran. However, we still believe much higher viscosity changes can be obtained in these systems by appropriate choice of photoadditives. Several photoreversible organic molecules including spripyran derivatives and stilbenes might be used in combination with reverse wormlike micelles of lecithin/SDC. Here also, the key will be the differential interaction of the photoisoforms with the reverse micelles.

6.2.3. Encapsulation of Model Compounds by Reverse Vesicles

Since vesicles are containers that have an interior liquid core, they can encapsulate a variety of solutes such as drugs, cosmetic ingredients or agrochemicals. These solutes could then be released slowly and in a controlled manner through the vesicle bilayer. In case of hydrophobic molecules, we need to measure the encapsulation ability of reverse vesicles for different hydrophobic solutes such as nile red and cholesterol which are soluble in oil. The measurement can be executed by a chromatography column or centrifugation with using density difference between vesicles with encapsulated solute and free, unencapsulated solute in organic solvents.

In case of hydrophilic molecules, reverse vesicles are capable of encapsulating them in hydrophilic portion of reverse vesicle bilayers unless they remain in nonpolar solvents with precipitation. The encapsulation of hydrophobic molecules in reverse

vesicles can be more efficient and cost-effective than that of hydrophilic molecules in reverse vesicles since the passive encapsulation of hydrophilic compounds requires subsequent removal of nonencapsulated molecules by time-consuming and costly procedure.[21] In fact, our experiment has shown that hydrophobic dye such as certain amount of rhodamine can be encapsulated in DMPC/$GdCl_3$ reverse vesicles without any precipitation (**Figure 6.2**). As part of future work, we will examine more diverse materials to encapsulate in the reverse vesicles.

Figure 6.2. After adding hydrophilic dye (Rhodamine 0.05 mM) to reverse vesicles (18.5 mM DMPC and 12 mM $GdCl_3$) in cyclohexane, the sample remains homogenous and transparent in non-polar solvent. This indicates the entrapment of the dye in the reverse vesicle bilayers.

REFERENCES

[1] Israelachvili, J. N. *Intermolecular and Surface Forces*; Academic Press: New York, 1992.

[2] Lasic, D. D. *Liposomes: From Physics to Applications*; Elsevier: Amsterdam, 1993.

[3] Mukherjee, K.; Moulik, S. P.; Mukherjee, D. C. "Thermodynamics of micellization of aerosol ot in polar and nonpolar-solvents - a calorimetric study." *Langmuir* **1993**, *9*, 1727-1730.

[4] Willard, D. M.; Riter, R. E.; Levinger, N. E. "Dynamics of polar solvation in lecithin/water/cyclohexane reverse micelles." *Journal of the American Chemical Society* **1998**, *120*, 4151-4160.

[5] Dutt, G. B. "Does the onset of water droplet formation alter the microenvironment of the hydrophobic probes solubilized in nonionic reverse micelles?" *Journal of Physical Chemistry B* **2004**, *108*, 7944-7949.

[6] Dreher, F.; Walde, P.; Walther, P.; Wehrli, E. "Interaction of a lecithin microemulsion gel with human stratum corneum and its effect on transdermal transport." *Journal of Controlled Release* **1997**, *45*, 131-140.

[7] Kreilgaard, M. "Influence of microemulsions on cutaneous drug delivery." *Advanced Drug Delivery Reviews* **2002**, *54*, S77-S98.

[8] Luisi, P. L.; Scartazzini, R.; Haering, G.; Schurtenberger, P. "Organogels from Water-in-Oil Microemulsions." *Colloid and Polymer Science* **1990**, *268*, 356-374.

[9] Scartazzini, R.; Luisi, P. L. "Organogels from Lecithins." *Journal of Physical Chemistry* **1988**, *92*, 829-833.

[10] Schurtenberger, P.; Magid, L. J.; King, S. M.; Lindner, P. "Cylindrical Structure and Flexibility of Polymer-Like Lecithin Reverse Micelles." *Journal of Physical Chemistry* **1991**, *95*, 4173-4176.

[11] Shchipunov, Y. A. "Lecithin organogel - A micellar system with unique properties." *Colloids and Surfaces a-Physicochemical and Engineering Aspects* **2001**, *183*, 541-554.

[12] Tung, S. H.; Huang, Y. E.; Raghavan, S. R. "A new reverse wormlike micellar system: Mixtures of bile salt and lecithin in organic liquids." *Journal of the American Chemical Society* **2006**, *128*, 5751-5756.

[13] Tung, S. H.; Huang, Y. E.; Raghavan, S. R. "Contrasting effects of temperature on the rheology of normal and reverse wormlike micelles." *Langmuir* **2007**, *23*, 372-376.

[14] Hashizaki, K.; Taguchi, H.; Saito, Y. "A novel reverse worm-like micelle from a lecithin/sucrose fatty acid ester/oil system." *Colloid and Polymer Science* **2009**, *287*, 1099-1105.

[15] Eastoe, J.; Vesperinas, A. "Self-assembly of light-sensitive sufactants." *Soft Matter* **2005**, *1*, 338-347.

[16] Paulusse, J. M. J.; Sijbesma, R. P. "Molecule-based rheology switching." *Angewandte Chemie-International Edition* **2006**, *45*, 2334-2337.

[17] Ketner, A. M.; Kumar, R.; Davies, T. S.; Elder, P. W.; Raghavan, S. R. "A simple class of photorheological fluids: Surfactant solutions with viscosity tunable by light." *Journal of the American Chemical Society* **2007**, *129*, 1553-1559.

[18] Kuang, G. C.; Ji, Y.; Jia, X. R.; Li, Y.; Chen, E. Q.; Zhang, Z. X.; Wei, Y. "Photoresponsive organogels: an amino acid-based dendron functionalized with p-nitrocinnamate." *Tetrahedron* **2009**, *65*, 3496-3501.

[19] Wang, C.; Chen, Q.; Sun, F.; Zhang, D. Q.; Zhang, G. X.; Huang, Y. Y.; Zhao, R.; Zhu, D. B. "Multistimuli Responsive Organogels Based on a New Gelator Featuring Tetrathiafulvalene and Azobenzene Groups: Reversible Tuning of the Gel-Sol Transition by Redox Reactions and Light Irradiation." *Journal of the American Chemical Society* **2010**, *132*, 3092-3096.

[20] Kunieda, H.; Nakamura, K.; Evans, D. F. "Formation of reversed vesicles." *Journal of the American Chemical Society* **1991**, *113*, 1051-1052.

[21] Mollee, H.; De Vrind, J.; De Vringer, T. "Stable reversed vesicles in oil: Characterization studies and encapsulation of model compounds." *Journal of Pharmaceutical Sciences* **2000**, *89*, 930-939.

[22] Boettcher, C.; Schade, B.; Fuhrhop, J. H. "Comparative cryo-electron microscopy of noncovalent N-dodecanoyl- (D- and L-) serine assemblies in vitreous toluene and water." *Langmuir* **2001**, *17*, 873-877.

[23] Ebbing, M. H. K.; Villa, M. J.; Valpuesta, J. M.; Prados, P.; de Mendoza, J. "Resorcinarenes with 2-benzimidazolone bridges: Self-aggregation, self-assembled dimeric capsules, and guest encapsulation." *Proceedings of the National Academy of Sciences of the United States of America* **2002**, *99*, 4962-4966.

[24] Dominguez-Gutierrez, D.; Surtchev, M.; Eiser, E.; Elsevier, C. J. "Ru(II)-based metallosurfactant inverted aggregates." *Nano Letters* **2006**, *6*, 145-147.

[25] Xu, X. N.; Wang, L.; Li, Z. T. "Reverse vesicles formed by hydrogen bonded arylamide-derived triammonium cyclophanes and hexaammonium capsule." *Chemical Communications* **2009**, 6634-6636.

[26] Tung, S. H.; Lee, H. Y.; Raghavan, S. R. "A facile route for creating "Reverse" vesicles: Insights into "Reverse" self-assembly in organic liquids." *Journal of the American Chemical Society* **2008**, *130*, 8813-8817.

[27] Li, W.; Li, B.; Wang, Y. L.; Zhang, J.; Wang, S.; Wu, L. X. "Vesicular assemblies of modified Mn-12 single molecular magnets." *Chemical Communications* **2010**, *46*, 6548-6550.

[28] Hoffmann, H. Viscoelastic Surfactant Solutions. In *Structure and Flow in Surfactant Solutions*; Herb, C. A., Prud'homme, R. K., Eds.; ACS: Washington, DC, 1994; pp 2-31.

[29] Raghavan, S. R.; Kaler, E. W. "Highly viscoelastic wormlike micellar solutions formed by cationic surfactants with long unsaturated tails." *Langmuir* **2001**, *17*, 300-306.

[30] Shchipunov, Y. A.; Shumilina, E. V. "Lecithin Bridging by Hydrogen-Bonds in the Organogel." *Materials Science & Engineering C-Biomimetic Materials Sensors and Systems* **1995**, *3*, 43-50.

[31] Kaler, E. W.; Murthy, A. K.; Rodriguez, B. E.; Zasadzinski, J. A. N. "Spontaneous Vesicle Formation in Aqueous Mixtures of Single-Tailed Surfactants." *Science* **1989**, *245*, 1371-1374.

[32] Evans, D. F.; Wennerstrom, H. *The Colloidal Domain: Where Physics, Chemistry, Biology, and Technology Meet*; Wiley-VCH: New York, 2001.

[33] Kunieda, H.; Nakamura, K.; Infante, M. R.; Solans, C. "Reversed vesicles from biocompatible surfactants." *Advanced Materials* **1992**, *4*, 291-293.

[34] Tamai, N.; Miyasaka, H. "Ultrafast dynamics of photochromic systems." *Chemical Reviews* **2000**, *100*, 1875-1890.

[35] Minkin, V. I. "Photo-, thermo-, solvato-, and electrochromic spiroheterocyclic compounds." *Chemical Reviews* **2004**, *104*, 2751-2776.

[36] Hirshberg, Y.; Fischer, E. "Photochromism and reversible multiple internal transitions in some spiropyrans at low temperatures .1." *Journal of the Chemical Society* **1954**, 297-303.

[37] Hirshberg, Y. "Reversible formation and eradication of colors by irradiation at low temperatures - a photochemical memory model." *Journal of the American Chemical Society* **1956**, *78*, 2304-2312.

[38] Keum, S. R.; Hur, M. S.; Kazmaier, P. M.; Buncel, E. "Thermochromic and photochromic dyes - indolino-benzospiropyrans .1. uv-vis spectroscopic studies of 1,3,3-spiro(2h-1-benzopyran-2,2'-indolines) and the open-chain merocyanine forms - solvatochromism and medium effects on spiro ring formation." *Canadian Journal of Chemistry-Revue Canadienne De Chimie* **1991**, *69*, 1940-1947.

[39] Ercole, F.; Davis, T. P.; Evans, R. A. "Photo-responsive systems and biomaterials: photochromic polymers, light-triggered self-assembly, surface modification, fluorescence modulation and beyond." *Polymer Chemistry* **2010**, *1*, 37-54.

[40] Wojtyk, J. T. C.; Wasey, A.; Kazmaier, P. M.; Hoz, S.; Buncel, E. "Thermal reversion mechanism of N-functionalized merocyanines to spiropyrans: A solvatochromic, solvatokinetic, and semiempirical study." *Journal of Physical Chemistry A* **2000**, *104*, 9046-9055.

[41] Chibisov, A. K.; Gorner, H. "Photoprocesses in spiropyran-derived merocyanines." *Journal of Physical Chemistry A* **1997**, *101*, 4305-4312.

[42] Macosko, C. W. *Rheology: Principles, measurements and applications*; VCH Publishers: New York, 1994.

[43] *Neutron, X-Ray and Light Scattering: Introduction to an Investigative Tool for Colloidal and Polymeric Systems*; Zemb, T.; Lindner, P., Eds.; Elsevier: Amsterdam, 1991.

[44] Wagner, C. D. *Handbook of x-ray photoelectron spectroscopy*; Perkin Elmer Corp, Eden Prairie: [S.l.], 1979.

[45] Brown, W. *Dynamic light scattering : the method and some applications*; Clarendon Press, 1993.

[46] Dreiss, C. A. "Wormlike micelles: where do we stand? Recent developments, linear rheology and scattering techniques." *Soft Matter* **2007**, *3*, 956-970.

[47] Zaks, A.; Klibanov, A. M. "Enzyme-catalyzed processes in organic-solvents." *Proceedings of the National Academy of Sciences of the United States of America* **1985**, *82*, 3192-3196.

[48] Carvalho, C. M. L.; Cabral, J. M. S. "Reverse micelles as reaction media for lipases." *Biochimie* **2000**, *82*, 1063-1085.

[49] Akutsu, H.; Seelig, J. "Interaction of metal-ions with phosphatidylcholine bilayer-membranes." *Biochemistry* **1981**, *20*, 7366-7373.

[50] Altenbach, C.; Seelig, J. "Ca-2+ binding to phosphatidylcholine bilayers as studied by deuterium magnetic-resonance - evidence for the formation of a Ca-2+ complex with 2 phospholipidmolecules." *Biochemistry* **1984**, *23*, 3913-3920.

[51] Marra, J.; Israelachvili, J. "Direct measurements of forces between phosphatidylcholine and phosphatidylethanolamine bilayers in aqueous-electrolyte solutions." *Biochemistry* **1985**, *24*, 4608-4618.

[52] Huang, Y. X.; Tan, R. C.; Li, Y. L.; Yang, Y. Q.; Yu, L.; He, Q. C. "Effect of salts on the formation of C-8-lecithin micelles in aqueous solution." *Journal of Colloid and Interface Science* **2001**, *236*, 28-34.

[53] Bockmann, R. A.; Grubmuller, H. "Multistep binding of divalent cations to phospholipid bilayers: A molecular dynamics study." *Angewandte Chemie-International Edition* **2004**, *43*, 1021-1024.

[54] Cordomi, A.; Edholm, O.; Perez, J. J. "Effect of ions on a dipalmitoyl phosphatidylcholine bilayer. A molecular dynamics simulation study." *Journal of Physical Chemistry B* **2008**, *112*, 1397-1408.

[55] Terech, P.; Weiss, R. G. "Low molecular mass gelators of organic liquids and the properties of their gels." *Chemical Reviews* **1997**, *97*, 3133-3159.

[56] George, M.; Weiss, R. G. "Molecular organogels. Soft matter comprised of low-molecular-mass organic gelators and organic liquids." *Accounts of Chemical Research* **2006**, *39*, 489-497.

[57] Sangeetha, N. M.; Maitra, U. "Supramolecular gels: Functions and uses." *Chemical Society Reviews* **2005**, *34*, 821-836.

[58] Kline, S. R. "Reduction and analysis of SANS and USANS data using IGOR Pro." *Journal of Applied Crystallography* **2006**, *39*, 895-900.

[59] Pedersen, J. S. "Analysis of small-angle scattering data from colloids and polymer solutions: modeling and least-squares fitting." *Advances in Colloid and Interface Science* **1997**, *70*, 171-210.

[60] Raghavan, S. R.; Cipriano, B. H. Gel formation: Phase diagrams using tabletop rheology and calorimetry. In *Molecular Gels*; Weiss, R. G., Terech, P., Eds.; Springer: Dordrecht, 2005; pp 233-244.

[61] Raghavan, S. R. "Distinct Character of Surfactant Gels: A Smooth Progression from Micelles to Fibrillar Networks." *Langmuir* **2009**, *25*, 8382-8385.

[62] Fieser, L. F.; Harris, G. C.; Hershberg, E. B.; Morgana, M.; Novello, F. C.; Putnam, S. T. "Napalm." *Industrial and Engineering Chemistry* **1946**, *38*, 768-773.

[63] Mysels, K. J. "Napalm - Mixture of aluminum disoaps." *Industrial and Engineering Chemistry* **1949**, *41*, 1435-1438.

[64] Wang, X. R.; Rackaitis, M. "Gelling nature of aluminum soaps in oils." *Journal of Colloid and Interface Science* **2009**, *331*, 335-342.

[65] Terech, P.; Schaffhauser, V.; Maldivi, P.; Guenet, J. M. "Living polymers in organic-solvents." *Langmuir* **1992**, *8*, 2104-2106.

[66] George, M.; Funkhouser, G. P.; Terech, P.; Weiss, R. G. "Organogels with Fe(III) complexes of phosphorus-containing amphiphiles as two-component isothermal gelators." *Langmuir* **2006**, *22*, 7885-7893.

[67] George, M.; Funkhouser, G. P.; Weiss, R. G. "Organogels with complexes of ions and phosphorus-containing amphiphiles as gelators. Spontaneous gelation by in situ complexation." *Langmuir* **2008**, *24*, 3537-3544.

[68] Pedersen, U. R.; Leidy, C.; Westh, P.; Peters, G. H. "The effect of calcium on the properties of charged phospholipid bilayers." *Biochimica Et Biophysica Acta-Biomembranes* **2006**, *1758*, 573-582.

[69] Pabst, G.; Hodzic, A.; Strancar, J.; Danner, S.; Rappolt, M.; Laggner, P. "Rigidification of neutral lipid bilayers in the presence of salts." *Biophysical Journal* **2007**, *93*, 2688-2696.

[70] Hashizaki, K.; Chiba, T.; Taguchi, H.; Saito, Y. "Highly viscoelastic reverse worm-like micelles formed in a lecithin/urea/oil system." *Colloid and Polymer Science* **2009**, *287*, 927-932.

[71] Hashizaki, K.; Taguchi, H.; Saito, Y. "New Lecithin Organogels with Sugars of RNA and DNA." *Chemistry Letters* **2009**, *38*, 1036-1037.

[72] Filippov, A.; Oradd, G.; Lindblom, G. "Effect of NaCl and CaCl2 on the lateral diffusion of zwitterionic and anionic lipids in bilayers." *Chemistry and Physics of Lipids* **2009**, *159*, 81-87.

[73] Wolff, T.; Emming, C. S.; Suck, T. A.; Vonbunau, G. "Photorheological effects in micellar solutions containing anthracene-derivatives - A rheological and static low-angle light-scattering study." *Journal of Physical Chemistry* **1989**, *93*, 4894-4898.

[74] Lee, C. T.; Smith, K. A.; Hatton, T. A. "Photoreversible viscosity changes and gelation in mixtures of hydrophobically modified polyelectrolytes and photosensitive surfactants." *Macromolecules* **2004**, *37*, 5397-5405.

[75] Sakai, H.; Orihara, Y.; Kodashima, H.; Matsumura, A.; Ohkubo, T.; Tsuchiya, K.; Abe, M. "Photoinduced reversible change of fluid viscosity." *Journal of the American Chemical Society* **2005**, *127*, 13454-13455.

[76] Kumar, N. S. S.; Varghese, S.; Narayan, G.; Das, S. "Hierarchical self-assembly of donor-acceptor-substituted butadiene amphiphiles into photoresponsive vesicles and gels." *Angewandte Chemie-International Edition* **2006**, *45*, 6317-6321.

[77] Pouliquen, G.; Amiel, C.; Tribet, C. "Photoresponsive viscosity and host-guest association in aqueous mixtures of poly-cyclodextrin with azobenzene-modified poly(acrylic)acid." *Journal of Physical Chemistry B* **2007**, *111*, 5587-5595.

[78] Jiang, Y. G.; Wan, P. B.; Xu, H. P.; Wang, Z. Q.; Zhang, X.; Smet, M. "Facile Reversible UV-Controlled and Fast Transition from Emulsion to Gel by Using a Photoresponsive Polymer with a Malachite Green Group." *Langmuir* **2009**, *25*, 10134-10138.

[79] Chen, D.; Liu, H.; Kobayashi, T.; Yu, H. F. "Multiresponsive reversible gels based on a carboxylic azo polymer." *Journal of Materials Chemistry* **2010**, *20*, 3610-3614.

[80] Yagai, S.; Nakajima, T.; Kishikawa, K.; Kohmoto, S.; Karatsu, T.; Kitamura, A. "Hierarchical organization of photoresponsive hydrogen-bonded rosettes." *Journal of the American Chemical Society* **2005**, *127*, 11134-11139.

[81] Kumar, R.; Raghavan, S. R. "Photogelling fluids based on light-activated growth of zwitterionic wormlike micelles." *Soft Matter* **2009**, *5*, 797-803.

[82] Kumar, R.; Ketner, A. M.; Raghavan, S. R. "Nonaqueous Photorheological Fluids Based on Light-Responsive Reverse Wormlike Micelles." *Langmuir* **2010**, *26*, 5405-5411.

[83] Ueda, M.; Kim, H. B.; Ichimura, K. "Photocontrolled aggregation of colloidal silica." *Journal of Materials Chemistry* **1994**, *4*, 883-889.

[84] Tanaka, M.; Yonezawa, Y. "Photochemical regulation of the electrical properties of the novel planar bilayer lipid membrane incorporating spiropyran derivatives." *Journal of Physical Chemistry* **1996**, *100*, 5160-5162.

[85] Khairutdinov, R. F.; Hurst, J. K. "Photocontrol of ion permeation through bilayer membranes using an amphiphilic spiropyran." *Langmuir* **2001**, *17*, 6881-6886.

[86] Wohl, C. J.; Helms, M. A.; Chung, J. O.; Kuciauskas, D. "Phospholipid bilayer free volume analysis employing the thermal ring-closing reaction of merocyanine molecular switches." *Journal of Physical Chemistry B* **2006**, *110*, 22796-22803.

[87] Lee, H. Y.; Diehn, K. K.; Ko, S. W.; Tung, S. H.; Raghavan, S. R. "Can Simple Salts Influence Self-Assembly in Oil? Multivalent Cations as Efficient Gelators of Lecithin Organosols." *Langmuir* **2010**, *26*, 13831-13838.

[88] Sein, A.; Vanbreemen, J. F. L.; Engberts, J. "Emergence of a lyotropic lamellar phase - surfactant-aqueous phase contact experiments examined with a cryo-transmission electron-microscope." *Langmuir* **1995**, *11*, 3565-3571.

[89] Harroun, T. A.; Koslowsky, M.; Nieh, M. P.; de Lannoy, C. F.; Raghunathan, V. A.; Katsaras, J. "Comprehensive examination of mesophases formed by DMPC and DHPC mixtures." *Langmuir* **2005**, *21*, 5356-5361.

[90] Grasdalen, H.; Eriksson, L. E. G.; Westman, J.; Ehrenberg, A. "Surface-potential effects on metal-ion binding to phosphatidylcholine membranes - p-31 nmr-study of lanthanide and calcium-ion binding to egg-yolk lecithin vesicles." *Biochimica Et Biophysica Acta* **1977**, *469*, 151-162.